NASA Technical Memorandum 101054 USAAVSCOM Conference Publication 89-A-002

Applications of Flight Control System Methods to an Advanced Combat Rotorcraft

Mark B. Tischler, Jay W. Fletcher,
Patrick M. Morris, and George T. Tucker

July 1989

NASA
National Aeronautics and
Space Administration

US ARMY
AVIATION
SYSTEMS COMMAND
AVIATION RESEARCH AND
TECHNOLOGY ACTIVITY

NASA Technical Memorandum 101054 USAAVSCOM Conference Publication 89-A-002

Applications of Flight Control System Methods to an Advanced Combat Rotorcraft

Mark B. Tischler, Jay W. Fletcher, and Patrick M. Morris
Aeroflightdynamics Directorate, U.S. Army Aviation Research and Technology Activity
Ames Research Center, Moffett Field, California
George T. Tucker, Ames Research Center, Moffett Field, California

July 1989

National Aeronautics and Space Administration

Ames Research Center
Moffett Field, California 94035

US ARMY AVIATION SYSTEMS COMMAND

AVIATION RESEARCH AND TECHNOLOGY ACTIVITY
MOFFETT FIELD, CA 94035-1099

APPLICATION OF FLIGHT CONTROL SYSTEM METHODS TO AN ADVANCED COMBAT ROTORCRAFT

Mark B. Tischler, Jay W. Fletcher, and Patrick M. Morris*
US Army Aeroflightdynamics Directorate, AVSCOM
Ames Research Center, Moffett Field, California

George T. Tucker
Flight Operations Branch, NASA
Ames Research Center, Moffett Field, California

ABSTRACT

Advanced flight control system design, analysis, and testing methodologies developed at the Ames Research Center are applied in an analytical and flight test evaluation of the Advanced Digital Optical Control System (ADOCS) demonstrator. The primary objectives of this paper are to describe the knowledge gained about the implications of digital flight control system design for rotorcraft, and to illustrate the analysis of the resulting handling-qualities in the context of the proposed new handling-qualities specification for rotorcraft. Topics covered in-depth are digital flight control design and analysis methods, flight testing techniques, ADOCS handling-qualities evaluation results, and correlation of flight test results with analytical models and the proposed handling-qualities specification.

The evaluation of the ADOCS demonstrator indicates desirable response characteristics based on equivalent damping and frequency, but undesirably large effective time-delays (exceeding 240 msec in all axes). Piloted handling-qualities are found to be desirable or adequate for all low, medium, and high pilot gain tasks; but handling-qualities are inadequate for ultra-high gain tasks such as slope and running landings. Correlation of these results with the proposed handling-qualities specification indicates good agreement for the bandwidth boundaries, but suggests the need for more stringent limits on allowable phase-delay. Analytical models based on emulation (s-plane) techniques compare favorably with flight-extracted frequency-domain characteristics of the overall (end-to-end) ADOCS responses. Direct digital analysis procedures are shown to be necessary to characterize the intersample behavior of the actuator rate response.

INTRODUCTION

Advanced combat (scout/attack) rotorcraft must exhibit good handling-qualities over a diverse spectrum of operational missions. Precision flightpath and attitude control and inherent "tight" attitude stability are needed for nap-of-the-earth (NOE) and hovering flight, especially in degraded visibility and/or single pilot operations; whereas, for air-to-air combat, not only agility but high maneuverability are required. To meet these requirements, advanced combat rotorcraft will require multi-mode, high-gain, digital flight-control systems. Pilot inputs may be provided through multi-axis, side-stick controllers

Presented at Royal Aeronautical Society International Conference on Helicopter Handling Qualities and Control, London, UK, 15-17 Nov. 1988.

*Currently Test Pilot, United Technologies Sikorsky Aircraft.

electronically or optically linked only to a flight-control computer. A number of research aircraft (refs. 1-3) have been developed to examine technologies needed to achieve these requirements. Unfortunately, the gap between demonstrated rotorcraft flight-control technology and the handling-qualities requirements for advanced combat rotorcraft in high pilot-gain tasks (ref. 4) is still a considerable one. One largely elusive goal of advanced control system technology, as applied to modern rotorcraft, is to achieve high bandwidth and low time delay response characteristics for good overall handling qualities. Achieving this goal will require significant methodology improvements to the flight-control system at all stages of its design, implementation, and testing.

Research at the Aeroflightdynamics Directorate (AFDD), U.S. Army Aviation Research and Technology Activity, and the National Aeronautics and Space Administration (NASA) located at Ames Research Center (ARC) has focused on developing improved methods for the design and testing of advanced combat rotorcraft flight-control systems to help bridge this technology gap. A design methodology for advanced multi-variable model-following systems was developed and implemented on a CH-47 aircraft by Hilbert (ref. 5). An advanced multi-variable control design based upon Linear Quadratic Gaussian (LQG) theory was developed and implemented by Holdridge (ref. 6). Limitations on achievable bandwidth in rotorcraft flight-control systems were studied by Chen and Hindson (ref. 7). Key concepts in the analysis and design of high bandwidth digital flight-control systems for advanced combat rotorcraft were presented and illustrated in a comprehensive analytical study by Tischler (ref. 8). Flight testing methods have been developed especially for characterizing the response dynamics of highly augmented rotorcraft. These tools, based on frequency domain (ref. 9) and time domain (ref. 10), methods are being routinely used to verify the closed-loop performance of new control systems and have been included in the updated helicopter handling qualities-specification (ref. 4). Finally, a wide range of simulation and flight-test studies were conducted at ARC and in cooperation with the Canadian National Research Council as part of the development of the new specification (ref. 11).

These advanced flight-control system methods have been applied in a comprehensive evaluation of the Advanced Digital Optical Control System (ADOCS) demonstrator (fig. 1). The overall program objective of the ADOCS was to provide the technology base for the engineering development of an advanced battlefield-compatible flight-control system that: (1) enhances aircraft mission capability; (2) improves handling qualities; and (3) decreases pilot workload. The ADOCS program has provided an extensive base of experience on the design, testing, and analysis of a full flight-envelope advanced combat rotorcraft. Researchers at ARC have supported the ADOCS project with piloted simulation studies (refs. 12 and 13), flight-control analyses (refs. 8 and 14), and flight test evaluations.

The purpose of this paper is to illustrate the application of these advanced flight control system methodologies to the ADOCS demonstrator, with the primary objectives being to describe the knowledge gained concerning the implications of digital flight control design for rotorcraft, and to illustrate the analysis of the resulting handling qualities in the context of the new handling qualities specification. Accordingly, a general review of the ADOCS flight control system is given initially, with particular emphasis on the elements that are important to the design of such a digital control system for rotorcraft relative to the handling qualities. Flight test results are then reviewed, first in terms of the observed handling qualities and then in terms of closed loop aircraft characteristics determined using system identification procedures. On this basis, the identified characteristics are matched against the new handling qualities specifications and the predicted handling qualities thus obtained are compared with the flight results.

The authors wish to express their appreciation to the entire ADOCS test team of the Boeing-Vertol Company for the outstanding support provided during the flight test evaluations. The authors are especially grateful to Mr. Nick Albion and Mr. Steve Glusman for the many fruitful and frank discussions

during the authors' visits to Boeing, and their openness in reports and papers on the ADOCS design and development. Frequency-sweep testing and safety-pilot duties were performed with care and professionalism by Boeing pilots John Tulloch and Jim Hotelling. Finally, the authors are very appreciative of the support provided by Mr. Joseph Dickinson of the US Army Applied Technology Directorate (AATD), during the past 4 years, that made possible our involvement in the ADOCS program.

DESIGN AND ANALYSIS METHODS

This section reviews the attitude response specifications for combat rotorcraft, and discusses the implications on flight-control system design. An analysis of the ADOCS pitch channel is presented in detail to illustrate the important advanced flight-control system concepts.

Control-System Design Requirements and Implications for Combat Rotorcraft

Key design drivers for flight-control systems of advanced combat rotorcraft are the requirements to achieve high bandwidth and low time delay. The proposed specification defines these parameters from a Bode plot of the end-to-end attitude response to pilot inputs (fig. 2). As shown in figure 3, the minimum acceptable pitch bandwidth ranges from $\omega_{BW} = 1$ rad/sec for most fully attended tasks in clear visibility to $\omega_{BW} = 3.5$ rad/sec for ultra-high gain tasks such as target acquisition and air-to-air tracking. Although the proposed specification restricts the level of phase delay τ_p (a rough approximation to the equivalent system time-delay), considerable fixed-wing experience (ref. 15) as illustrated in figure 4 suggests that the allowable levels of time delay, especially for the ultra-high tasks (fig. 3), are too large. However, success in achieving even the proposed bandwidth and time delay requirements for rotorcraft is limited by a number of fundamental factors to rotorcraft digital flight-control implementation as is now discussed.

A generic digital-control implementation is shown in figure 5 for the pitch channel as an example. Pilot command inputs from a multi-axis, side-stick controller (δ_s) are filtered and then sampled before being passed to the digital flight computer. The command path contains selectable response shaping modes (e.g., attitude command or rate command) and feedforward dynamics to improve control-response bandwidth. The digital feedback signals are obtained from onboard sensors, which are filtered to prevent aliasing of high-frequency noise, and are then sampled and shaped through digital feedback compensation. Forward-loop compensation provides the desired open-loop response characteristic (δ_f/e) and crossover frequency (ω_c). Notch filter compensation may also be required in the forward stabilization path or command path to eliminate undesirable biodynamic interference, which has been a recurring problem associated with side-stick controllers in rotorcraft (refs. 2 and 16) and fixed-wing aircraft (ref. 8). The digital computer is coupled to control surface actuators through a digital-to-analog converter (usually a zero-order hold), which introduces delays and high-frequency actuator ripple. Finally, the rotor and actuators dominate the high-frequency dynamics in rotorcraft flight-control systems. In hovering flight, the effective rotor system bandwidth is about 15 rad/sec (as discussed later in this section); this frequency may only be three or four times greater than the closed-loop bandwidth, and will thus have a significant impact on the achievable response characteristics.

The maximum closed-loop bandwidth for the control system of figure 5 is therefore limited by a number of factors: (1) sensor noise amplification, (2) rotor and inflow dynamics, (3) phase-margin

requirements and high-frequency modeling uncertainty (flexible structure modes), and (4) actuator limiting (position and rate).

Historically, the phase-margin requirement has put the greatest restriction on achievable system bandwidth. The design values of open-loop crossover frequency (ω_c) and phase-margin (Φ_m) limit the allowable phase-lag contributions from the various high-frequency elements in the stabilization loop (δ_f/e, fig. 5), including the filters, actuators, and rotor system.

Simple, but very useful, design plots and guidelines have been developed which illustrate the fundamental control system considerations. Such simple rules are possible because the required closed-loop bandwidth is generally at a much higher frequency than the open-loop rigid-body modes and at a lower frequency than the rotor and actuator modes. Consider the following example requirements for an ultra high-gain, pilot-in-the-loop task:

$$\omega_{BW} = 3.75 \text{ rad/sec (from fig. 3)}$$

$$\tau_e = 0.150 \text{ sec (from fig. 4)}$$

Figure 6 developed by Blanken (AFDD) shows the effect of equivalent time delay (τ_e) on the bandwidth (ω_{BW}, 45° phase margin definition) of a second order attitude response system (for $\zeta = 1.0$), like that of the example control system in figure 5. The plot indicates that a closed-loop natural frequency of 3.0 rad/sec is required to achieve the desired bandwidth level and time delay. From a classical design standpoint, this implies that an open-loop crossover frequency of $\omega_c = 3.0$ rad/sec is required. Notice that the associated phase delay $\tau_p = 0.11$ sec is substantially less than the 0.2 sec maximum value allowed in the specification. As derived in reference 8, the achievable crossover frequency depends linearly on the effective time delay τ_{SL} in the stabilization loop (δ_f/e of figure 5):

$$\omega_c = \frac{0.370}{\tau_{SL}} \qquad (1)$$

which indicates a maximum allowable stabilization loop delay of $\tau_{SL} = 0.123$ sec for $\omega_c = 3.0$ rad/sec.

The most important contributors to the stabilization-loop equivalent time delay for a rotorcraft digital control system are (in descending order):

1. Rotor response
2. Actuator dynamics
3. Filters: sensor and anti-alias
4. Sample and hold delay
5. Computational delay
6. Discrete (e.g., Tustin) transform approximation

As shown by Heffley (ref. 10), rotor delays are approximated by the value of $\gamma\Omega/16$, which does not vary more than about 10% for a wide range of helicopter rotor types including hingeless, articulated,

and teetering. Based on the UH-60 rotor delay of 66 msecs (which implies a rotor bandwidth of about 15 rad/sec), this illustrates that the rotor system alone accounts for a roughly invariant 50% of the total allowable stabilization loop time delay. Increasing the rotor system bandwidth using rotor-state feedback control shows the potential for significant reduction in this major source of overall time delay. Current technology actuators have equivalent time delays of about 20 msec, leaving an allocation of 38 msec for the remaining elements in the stabilization loop (anti-alias noise filter, notch filter, ZOH, computational delay). These elements can be implemented using a sample rate of 60 Hz, which is a typical value for current fixed-wing technology. The delays of all of the forward-path elements of the stabilization loop ($\delta_{f/e}$, in fig. 5) contribute directly to the overall command response delay. Feedback path filters ($\tau = 0.014$ anti-alias/noise filter) do not contribute significantly to the command response delay, so the total contribution from the stabilization loop is $\tau = 0.123 - 0.014 = 0.109$ sec. Referring to the allowable overall delay of $\tau_c = 0.150$ sec, this leaves a remaining allocation of 41 msec for the command loop elements, which is sufficient to implement the necessary stick filter and account for stick sampling skew. As is seen in this example, the design requirements are achievable with current rotorcraft technology, but require careful allocation of time delays in the system.

The goal of achieving high bandwidth control systems for rotorcraft has remained illusive largely because the time delays have not been tightly allocated and monitored in the design process. For example, the original ADOCS design featured a 6 rad/sec crossover frequency in the pitch axis with an associated equivalent time delay of $\tau_c = 147$ msec (ref. 17). However, many practical implementation elements were not included in this original control system design. Table 1 shows an average overall 51% reduction in gain from the original ADOCS simulation design of 6 rad/sec, through initial flight tests and flight control system optimization. The measured pitch crossover frequency of 2.44 rad/sec and equivalent time delay of $\tau_c = 238$ msec for the optimized flight configuration shows how these practical implementation considerations can degrade system performance.

Advanced Flight-Control System Design and Analysis Based on the ADOCS Concept

This section presents an overview of the ADOCS concept and an analysis of the pitch channel using flight values of the control system parameters.

ADOCS Concept– The ADOCS model-following concept is shown generically in figure 7. This architecture uses feedforward and inverse plant dynamics to cancel the inherent rotorcraft dynamics and replace them with the desired command responses. A key advantage of this explicit model-following approach is the capability to independently set the command and stabilization response characteristics, thus providing multi-mode handling qualities as is required for the scout/attack (SCAT) mission. For example, an attitude command response may be desired for low-speed flight in degraded visibility conditions, while a rate command system may be desirable for flight in unrestricted visibility conditions. In both environments, a high degree of attitude stabilization is desirable. In the actual ADOCS implementation, the block diagram of figure 7 is rearranged somewhat to separate the system into two digital paths. One path, the "primary flight control system" (PFCS), contains only feedforward elements and serves as a high-reliability backup system. The other path, the "automatic flight-control system" (AFCS), contains both feedforward and feedback elements. In the fully operational state, both paths are active, and the response characteristics simplify to those of figure 5. Therefore, the distinction between the PFCS and AFCS is not important to this study.

Reference 8 presents a comprehensive case study of an advanced hover/low-speed flight-control system for the UH-60 based on the ADOCS concept using design values for the important parameters.

Analog methods are used to illustrate the degradation in control system performance resulting from the various practical implementation aspects discussed earlier. Analog and direct digital methods were used to evaluate control system performance for a nominal 30 Hz operational system and a backup 15 Hz design. The following discussion presents updated results of the analysis of the pitch channel based on the actual flight test values of the control system parameters. Analytical and flight test results are compared later in this paper.

Pitch Axis Characteristics Using s-Plane Analysis Techniques– Analysis techniques based on analog (s-plane) control theory are very useful in evaluating the overall end-to-end performance of a moderate sample rate control system, such as the ADOCS. A block diagram of the flight-test configuration pitch axis channel for hover is shown in figure 8. (Once again the distinction between the PFCS path and AFCS path is not important for analyzing the fully functioning system.) The forward stabilization loop contains the helicopter rigid-body response, the ADOCS and upper-boost actuators, and the rotor dynamics. Each of these elements is represented by high-order transfer function models that are given in reference 8. For illustration, the equivalent time delay of each of these elements is indicated in the figure. Feedback gains for the current flight evaluation are given in table 1. The command loop contains several nonlinear elements (dead zone, nonlinear stick sensitivity function, derivative rate-limiter) that are ignored in the present analysis. The command model for the pitch channel in hover is a second-order, 2-rad/sec, attitude response with a 5-sec trim rate follow-up to alleviate steady trim-force requirements (table 2). Note that the sum of the delays indicated in figure 8 for the ADOCS flight configuration is considerably larger than the values allowed in the previous section for achieving desirable combat rotorcraft specifications ($\omega_{BW} = 3.75$ rad/sec, $\tau_e = 0.150$ sec). The following analysis is presented to show the resulting effect on the flight system performance.

The equalized open-loop frequency-response of the stabilization path (δ_f/e) is shown in figure 9. The crossover frequency is $\omega_{c\theta} = 2.75$ rad/sec, with an associated phase margin $\Phi_m = 55°$ and a gain margin of GM = 11.76 dB. Referring to figure 8, the total stabilization-loop time delay is $\tau_{SL} = 0.165$ sec. The simple design rule of equation (1) predicts an achievable crossover frequency of $\omega_{c\theta} = 2.24$ rad/sec, which is close to the true value.

A root locus plot varying stabilization loop gain is presented in figure 10 using the higher-order transfer functions for all system elements. The open-loop rigid-body modes are seen to be well sup pressed, even for this fairly moderate design crossover frequency. The location of the dominant closed-loop mode at 2 rad/sec is determined almost entirely by the location of the compensation zero at 1.54 rad/sec, associated with the ratio of pitch attitude and pitch rate gains. These closed-loop conditions are often referred to as "super augmentation" (ref. 2). As can also be seen in the figure, the bandwidth is limited by the destabilization of the regressing flapping mode.

The frequency response of the normalized end-to-end transfer function θ/δ_s is co-plotted with the response of the command model alone θ_m/θ_c in figure 11. The match between these responses is a good measure of the model-following performance of the system. Acceptable magnitude response following is maintained out to about 10 rad/sec. At higher frequencies, following degrades because the rotor dynamics are not included in the inverse model P^{-1} (ref. 8). Phase response following degrades at a much lower frequency because the time delays in the control system are not included in the command model.

The pitch attitude response to a step input in hover is shown in figure 12. The attitude continues to increase monotonically during (and beyond) the first 4 sec of the response, due to the trim rate follow-up. Therefore, despite having an "attitude command model," the ADOCS is characterized by the handling qualities specification as a rate response type (ref. 4). As such, the bandwidth frequency is defined the

lesser of the 45° phase margin frequency or the 6 dB gain margin frequency. From figure 11, the system is gain-margin limited with a bandwidth of $\omega_{BW_\theta} = 2.48$ rad/sec. The associated phase delay obtained from the figure is $\tau_{p_\theta} = 0.179$ sec. Reference to the pitch response specification of figure 3 indicates that the ADOCS should achieve Level 1 handling qualities in all but the most severe tasks.

The end-to-end frequency response of figure 11 is well characterized by a second-order equivalent system model fit in the frequency range of 0.1 – 10.0 rad/sec:

$$\frac{\theta}{\delta_s} = \frac{5.26(s + 0.2)e^{-0.244s}}{s[0.964,\ 2.35]} \tag{2}$$

(Shorthand notation; $[\zeta, \omega]$ implies $s^2 + 2\zeta\omega s + \omega^2$.)

Comparison of the equivalent system model of equation (2) with the handling qualities data of reference 18 is shown in figure 13. The results indicate desirable command response characteristics based on damping ratio and natural frequency. However, reference to figure 4 suggests that the equivalent time delay of 244 msec will result in marginal Level 2/Level 3 handling qualities (HQR 6-7) for high stress pitch tasks. The breakdown of contributions by the various forward loop elements to the total equivalent system time delay is summarized in table 3. (The difference between the equivalent delay of eq. (2) and the total of table 3 is due to fit mismatch.) Clearly the rotor, actuators, and filter dynamics are dominating the large time delay, as discussed earlier. The stick skewing and zero-order hold delays are a small fraction of the total value. Notice that the sensor filter is not included in table 3 since elements in the feedback path do not substantially contribute to the command response time delay.

This completes the overview of the ADOCS pitch channel. Additional analytical results are presented in references 8 and 14.

FLIGHT TESTING TECHNIQUES

The ambitious, multi-roled mission of the advanced combat rotorcraft has resulted in a significant rise in system complexity, and has demanded a complete re-thinking of the approach to handling-qualities evaluation and helicopter flight testing. Considerable emphasis must be placed on pilot familiarization to achieve the necessary level of training with new devices such as multi-axis sidestick controllers, advanced augmentation systems, automatic and manual mode switching, and subtle digital transient problems. Many of the classical handling-qualities tests such as stick-free stability, and stick position versus speed may be meaningless because of isometric controllers, rate command response types, and high levels of feedback stability. Quantitative time-domain testing techniques based on steps and pulses are not sufficiently sensitive to equivalent time delays to expose potentially serious latent pilot-induced oscillation (PIO) tendencies, and do not provide accurate measurement of bandwidth (refs. 8 and 19). Therefore, a comprehensive frequency-domain based technique using frequency sweeps and advanced system identification procedures has been developed and incorporated in the new specification.

The ADOCS program has provided an excellent opportunity to evaluate advanced flight control design and flight test techniques on a state-of-the-art combat rotorcraft. The primary objectives of the evaluation that is summarized here were to:

1. Evaluate the basic ADOCS handling qualities characteristics for the AFCS in hover, low-speed, and cruise flight.

2. Quantify the end-to-end performance of the AFCS.

3. Correlate handling-quality ratings and comments with quantitative response characteristics to provide guidance for future control system development.

4. Correlate findings with the new handling-qualities specifications.

During this (final) phase of AFDD evaluation, top priority was given to fully evaluating a 3+1 (collective) control configuration with a newly implemented displacement collective, followed by an evaluation and comparative assessment of the recently modified force collective configuration (fig. 14). System difficulties prevented evaluation of the 4+0 configuration. Results presented here are confined to those obtained with the displacement collective configuration. Flight hour distribution is presented in table 4.

Prior to commencement of the flight evaluation, a set of frequency sweeps in each control axis was conducted on the ground with rotors stationary to familiarize the Boeing pilots with the desired input technique. As with the in-flight frequency sweeps which followed, the real-time control input data was transmitted to the ground data station for evaluation of amplitude and frequency content by the test engineer.

The final phase handling qualities evaluation was structured for one AFDD evaluation pilot flying maneuvers from the same basic test card of hover, low-speed, and up-and-away tasks on sequential flights. The assessment was structured to progress from primarily single-axis tasks to those requiring simultaneous control of four axes to provide a measure of the pilot learning curve on the sidearm controllers while obtaining the necessary pilot ratings. NOE, air-to-air, and PFCS-only tasks evaluated during the previous evaluations were not repeated here. Winds for all tasks were steady at speeds ranging from calm to 12 knots (variable at 6-8 knots for the most part). Handling Qualities Rating(s) (HQR) were assigned to the tasks according to the methods and definitions contained in reference 20.

The primary AFCS configuration for both frequency sweep testing and the handling qualities evaluation was the core AFCS with heading hold engaged (table 5). The additional capabilities provided by the Hover Hold, Velocity Stabilization, and Radar and Barometric Altitude Hold modes were used selectively in the handling qualities evaluation when considered appropriate for the task.

Handling Qualities Evaluation

Side-stick controller implementations have generally demonstrated a degradation in HQRs as the "pilot gain" required to accomplish a task has increased. Increasing pilot gain, as used here, is indicated when the required precision of the task, as perceived by the pilot, forces an increase in control input frequency. The discussion of results obtained from the current experiment is therefore presented with respect to the low, medium, high, and ultra-high gain nature of the individual tasks. The tasks evaluated are listed in tables 6-9 with comments regarding either the major focus of pilot workload or enhancing characteristics and the associated HQRs.

Low Gain Tasks

This category of task is characterized by attitude and velocity stability which produces a "hands-off" (or near hands-off capability), or low pilot workload in the primary control axis. The present configuration of the ADOCS appears optimized for the hover and low speed environment where the aircraft flies best with a minimum of pilot input. Handling Quality Ratings were Level 1 for all tasks (table 6).

Cruise Flight– In up-and-away cruise flight the aircraft was well stabilized for constant attitude and airspeed. Direct control of collective pitch though the displacement collective resulted in good control of vertical rates. Steady state roll rate was quite reasonable, with rollout accuracies of 2-3° at near maximum rates. Maintenance of roll attitude in constant bank angle turns greater than 2-3° was excellent, as was the directional trim. When returned to a near wings level attitude of less than 3°, the aircraft rolled to a steady state 2-3° bank angle in either direction, with the ball approximately 1/2 out in the opposite direction.

Precision Hover– At hover in steady winds up to 12 knots, the aircraft was very stable in attitude with little resulting tendency to drift at altitudes from barely above touchdown to out-of-ground effect. Pilot workload was largely unaffected by wind azimuth at these velocities. 360° turns at 20-25°/sec were executed with relative ease. Use of hover mode, velocity stabilization, and radar altitude hold modes generally improved the HQRs by one rating for most hover tasks. Heading control for large amplitude turns at aggressive rates was a bit jerky with heading hold engaged and a bit imprecise when stopping without heading hold selected. Hover performance was evaluated over concentric circles of 10, 54, and 108 ft in diameter painted on a taxiway.

Medium Gain Tasks

Medium gain tasks are characterized by significant pilot effort in a minimum of two control axes accompanied by an increase in the pilot attention dedicated to assessment of maneuver precision. Roll and yaw coordination account for the major portion of the workload in the tasks discussed here. Handling Qualities Ratings were borderline Level 1/Level 2 (table 7).

Lateral-Directional Tasks– The "Hover Circle" is primarily a lateral-directional task in which the aircraft translates in sideward flight at a constant altitude around a circle, painted on the ground, equal in diameter to the main rotor while continuously keeping the nose pointed at circle center. Workload in the vertical and lateral axes was low, which accentuated the added effort required to continuously and smoothly yaw the aircraft against the heading hold. Deselecting the heading hold caused the yaw axis to revert from rate command/heading hold to acceleration command with rate stabilization, resulting in increased ease of input in the yaw axis and a jump in the HQR from 4 to 2.5.

The 15 knot Slalom task further increases the lateral-directional coordination required while increasing the effort required in the longitudinal axis for control of air/groundspeed. The task required that the pilot fly to and around lights that were spaced 300 ft apart longitudinally on alternate sides of a runway 200 ft wide. The elevated pilot workload in the yaw axis was moderated by deselecting heading hold. This produced a smoother, less jerky maneuver at the expense of reduced directional stability.

Pilot workload in sideward flight was predominantly in the roll axis with some smaller amount of effort required in yaw. Accuracy of roll attitude control near maximum roll rate was slightly less than desired due to the pilot's inability to predict the size and timing of the input for large amplitude, high fre-

quency tasks. Constant heading, within 2-3°, was maintained during lateral translations to 30 knots with heading hold selected regardless of the level of the aggressiveness.

Directional Tasks– A target switch-off task was executed from the hover between targets 30° apart with radar altitude hold selected in addition to core AFCS plus heading hold. Yaw rates of 20-25°/sec were generated with overshoots not exceeding 2° followed by a rapid return to target (HQR 3). With heading hold deselected the ease of maneuver entry was increased only slightly at the expense of significantly degraded target acquisition.

Vertical Tasks–The bob-up task, consisting of an aggressive climb from 20 to 75 ft AGL, followed by a return to 20 ft, after a pause of 2-3 sec, was accomplished with good vertical rates and satisfactory heave damping. Longitudinal and lateral hover positions were maintained within the 10 ft hover circle painted on the ground.

180° Return to Target– This maneuver consists of an aggressive turn entry to 45° of bank from level flight at 80 kias. After 180° of turn the wings are aggressively leveled, and the nose rapidly fixed and held on a target 15° below the horizon. The nose is held on target for 3 sec before being returned to level flight. Roll in and out was smoothly and accurately accomplished, on speed with the ball held centered throughout the turn. The nose was very easy to hold on the target and could have been held considerably longer (HQR 3).

High Gain Tasks

High gain tasks require significant control activity in 3 or 4 of the control axes simultaneously, or in a lesser number of axes near the maximum capacity of the pilot. These tasks received HQRs consistently in Level 2 as shown in table 8.

Lateral Escape– The lateral escape maneuver requires the pilot to translate laterally to an estimated 20 knots of ground speed before simultaneously rotating and lowering the nose to accelerate into forward flight at a 90° angle to the initial heading. The climb and acceleration at 80-90% power are continued until reaching 80 knots followed by a 180° turn at 40-50° of bank in the direction of the initial lateral translation. This maneuver was reasonably straightforward with good lateral and longitudinal control of acceleration. However, with heading hold engaged, the aircraft was excessively stiff directionally requiring considerable effort to get the aircraft yawed 90° at low speed (HQR 6). With heading hold deselected, the new heading was achieved with much less effort (HQR 4) with no noticeable degradation in other aspects of the overall task.

Normal Vertical Landing from Hover– In spite of the general simplicity of the maneuver, the basic landing task demonstrated the characteristics of a high gain task. The workload during the descent from hover was very low, exhibiting excellent Level 1 characteristics. However, just prior to virtually all touchdowns, a persistent 1 Hz lateral Pilot-Induced Oscillation (PIO) (fig. 15) was observed on the telemetry data, but was not necessarily apparent to the pilot. Generally, the lateral oscillation subsided in the process of getting all the gear on the ground. For those situations where the landing was accomplished without a DOCS monitor trip, the HQRs varied between 4 and 5. The lift-off to a hover was generally one HQR worse than the landing due to the inability to precisely modulate roll attitude during the period when the aircraft is becoming light on the landing gear.

Dash/Quickstop– The level acceleration to 50-60 knots was generally accomplished with some slight sluggishness in pitch and a small amplitude roll oscillation in the 30-40 knot airspeed range, but still within Level 1. Typically, the flare produced a yaw slice to the right with several cycles of lateral 1 Hz PIO before the nose attitude was again level at a hover (HQR 4-6).

30-Knot Slalom– The handling qualities difficulties were very similar to those during the 15-knot slalom but elevated by a perceived increase in overall control activity of 50%, a more jerky response when coordinating yaw requirements (heading hold selected), and the characteristic sluggishness longitudinally (HQR 4.5-5). With heading hold deselected the lateral-directional task workload was reduced slightly.

Ground Taxi– Longitudinal cyclic control via direct input from the controller or the "beeper trim" switch was difficult to modulate with precision. Tip-path plane response to the beeper seemed slow and without sufficient visual feedback to readily control taxi speed. Precision of directional control was generally satisfactory for small heading changes but inadequate for modulating large changes or rapid heading reversals. HQRs varied from 3 to 9, increasing with complexity and required precision of the maneuver.

Ultra-High Gain Tasks

The slope landings and running landings are examples of tasks which required control input at the maximum capacity of the pilot. These tasks received HQRs in the Level 2/Level 3 areas as shown in table 9.

Slope Landings– Slope landings were attempted, both left- and right-wheel-upslope, at angles of 3-8°. The 8° slope task was accomplished in a box painted on the ground measuring 13 by 32 ft. Left-wheel upslope landings were consistently accomplished with low workload through touchdown of the tail and left main gear. The process of lowering the right main to the ground produced occasional overcontrolling in yaw and an ever-present and sometimes divergent 1 Hz lateral oscillation in roll (HQR 4-5). Liftoffs from the slope landings were characteristically 1 HQR worse than the landing due to the inability to smoothly modulate the changing lateral control requirements from full weight on the gear to liftoff. Right-wheel upslope landings to the 8° slope were not possible due to repeated divergent directional and lateral PIOs (fig. 16).

Running Landings– The evaluation pilot was unable to complete a landing, tailwheel-first without a DOCS monitor trip at first tailwheel contact. Running landings in a flat attitude at approximately 15 knot ground speed were complicated by the inability to make precise, corrective directional control inputs to ensure proper alignment of the fuselage just prior to ground contact. Directional inputs became oscillatory (fig. 17) with the pilot inadvertently coupling directional inputs into the roll axis (HQR 8).

DATA ANALYSIS TECHNIQUES

The on-board PCM data was analyzed to allow flight response comparisons with analytical models, the proposed handling-qualities specifications, and the pilot ratings and comments. The focus of the effort was in the extraction of frequency responses and transfer-function models.

A flow chart of the data analysis procedure used to perform the small-amplitude control response documentation of the ADOCS demonstrator is shown in figure 18 and is described in detail in reference 9. Spectral analysis of the pilot control and motion variable time histories were performed by the frequency response identification program FRESPID to produce end-to-end frequency responses in Bode plot form. The bandwidth and phase delay parameters were then calculated directly from the attitude frequency response plots. Transfer function models were generated from least squares fits of the Bode plots using the program NAVFIT for comparison with analytically developed transfer function models. The time domain response of the identified models and the flight data were compared for the same pilot inputs to provide further verification of the identification.

Identification of frequency responses and transfer function models of the bare airframe dynamics by the above methodology was also completed using swash plate deflections instead of side stick deflections as the input time histories.

A typical pilot control frequency sweep in hover of the longitudinal side-stick is shown in figure 19a. The sweep begins with the aircraft in trim and progresses smoothly from low frequency to high frequency, with off-axis inputs used as necessary to keep the aircraft oscillating roughly about trim. The pitch rate of the aircraft during this frequency sweep is shown in figure 19b. This signal, like the pilot input, should start and end in trim and be roughly symmetrical about trim for the duration of the sweep. In this case the angular rate signal was used because its frequency content is better suited for identification of the phase curve at high frequency from which the phase delay parameter is calculated. A simple 1/s correction of the angular rate frequency response was performed to yield the attitude frequency response for calculation of the bandwidth and phase delay.

Several frequency sweeps in each axis, flight condition and vehicle configuration were flown to ensure that at least two good records were available for concatenation so that a high quality identification could be obtained. The pitch rate frequency response to longitudinal side-stick for six concatenated sweeps is shown in figure 20 for the hover flight condition. The rate-response nature of the aircraft at frequencies below 0.4 rad/sec due to the trim rate follow-up is evident as is the dominant second-order mode near 2 rad/sec. The phase curve is shifted down by 180° because of the stick deflection sign convention. For frequencies above 7 rad/sec, the sudden flattening of the phase curve and the oscillations in both the magnitude and phase curves suggests declining identification accuracy.

The coherence function, γ^2 (shown in fig. 21), is a measure of the extent to which the input supplied to FRESPID is linearly related to the output. Drops in its value below unity can result from nonlinearities, off-axis inputs, disturbance inputs (gusts, turbulence), low input power (insufficient excitation of the vehicle) or sensor noise. Coherence function values below 0.8 or rapid oscillation of the coherence curve are generally indicative of poor frequency response identification. In this case the rapid decrease in coherence above 7 rad/sec confirms earlier suspicions about poor identification in this region.

The coherence function and the number of concatenated sweeps are used to determine the normalized random error, ε_r, described in reference 21. This parameter is a direct measure of identification accuracy. Lower values are indicative of higher coherence (low noise) and more concatenated time histories (increased information). The random error for the pitch rate response to longitudinal side-stick, $\varepsilon_{\delta_{LON}q}$, shown in figure 22, indicates accurate identification in the frequency range of 0.21 to 7 rad/sec (less than 5%).

The $\theta/-\delta_{LON}$ frequency response shown in figure 23 is obtained from the q/δ_{LON} frequency response by applying a simple 1/s correction and a sign change (to yield positive pitch to longitudinal

side-stick). Illustrated in figure 23 are the calculations of the bandwidth and phase delay for the longitudinal axis in hover. It can be seen that since this is considered a rate system, the bandwidth is slightly gain-margin limited at $\omega_{BW_\theta} = 2.10$ rad/sec. The phase delay calculation occurs in a frequency range where the phase curve is smoothly rolling off and where the quality of the identification is considered to be sound, so no least squares extrapolation of the phase curve is necessary (see ref. 9) and confidence in the calculated value of $\tau_{p_\theta} = 0.202$ is high.

The bandwidths and phase delays calculated for the longitudinal, lateral and directional axes in hover and at 80 knots are displayed in table 10. The directional results are for sweeps of the force pedals, since these data are of higher quality than the directional side-stick sweeps. The only difference between the pedals and directional side-stick is in the overall gain (not important), which does not affect the bandwidth, phase delay, transfer function, or time delay. The results for the longitudinal and lateral axes in hover are quite similar as one would expect since the command models (table 2) and rotor dynamics in these two axes are quite similar. Both bandwidths are slightly gain margin limited as is the bandwidth for the yaw axis in hover. The phase delay for the yaw axis in hover is smaller than those in the other axes because of the smaller time delays associated with the tail rotor dynamics.

The bandwidth and phase delay parameters calculated for the pitch axis at 80 knots are similar to those calculated at hover. This is to be expected since the pitch axis command model is unchanged between hover and 80 knots. The command model for the roll response, however, changes from attitude command to rate command for the 80-knot flight condition. The rate response type combined with large time delays cause a significant drop in the gain margin bandwidth ($\omega_{GM} = 0.94$ rad/sec). The phase delay calculated for the roll axis at 80 knots is similar to that calculated for the hover flight condition indicating good modeling by this parameter of high frequency delays which are nearly invariant with advance ratio. A similar result is noted in the pitch axis. The cause of the large increase in phase delay from hover to 80 knots in the directional axis, however, is unknown.

Transfer function models were fit with the program NAVFIT to the identified angular rate frequency responses using the same forms as the command models (table 2). The frequency ranges of each fit were selected to correspond to the range of low random error in the frequency-response identification.

The results are shown in table 10 for the hover and 80-knot flight conditions along with their frequency ranges of applicability. The pitch rate due to longitudinal side stick models at hover and 80 knots have nearly the same natural frequency and both are slightly less than the command model's natural frequency of 2 rad/sec. The slightly higher natural frequency for the roll rate response to lateral side-stick in hover is consistent with the slightly larger bandwidth seen in this axis before. The identified corner frequency for the roll rate response at 80 knots is significantly lower than that of the command model as was indicated before by the low bandwidth in this axis. Identified time delays in the longitudinal and lateral axes are roughly constant between flight conditions and axes as expected.

In the directional axis, the identified time delay and corner frequency of the first-order rate response both increase from hover to 80 knots. This is consistent with the increases in bandwidth and phase delay from hover to 80 knots mentioned earlier.

Verification of the transfer function models was performed by driving state-space representations of the models with pilot generated step inputs measured in flight and comparing the model response to the measured vehicle response. It was sometimes necessary to vary the transfer function gain to account for the differing effects that the nonlinear shaping had on the step and sweep type inputs and on inputs of different size.

Time histories of a longitudinal side stick step input in hover along with comparisons of the model and vehicle attitude and rate responses are shown in figure 24. A gain reduction of 10% was introduced to achieve the excellent pitch rate matching shown in the figure. The resulting pitch angle comparison is also very good. Good matching of the initial slopes and general dynamic characteristics of the curves is indicative of a good transfer function model. The slight mismatch in the attitude response beginning at 13 sec is likely to have been caused by a disturbance input.

DISCUSSION OF RESULTS

This section first compares the identified and analytical design models of the component and end-to-end system performance. Then, the handling-quality ratings and comments are correlated with the analytical models and the proposed specification requirements.

Comparison of Identified and Analytical Models

An identification of the basic (unaugmented) UH-60 in hover was completed using the measured ADOCS actuator signal as the input and the aircraft pitch rate as the output. Therefore, the resulting frequency response shown in figure 25 reflects the dynamics of the UH-60 airframe, rotor, and upper-boost actuator. Also shown in figure 25 is the frequency response of the analytical transfer-function models from figure 8. The associated coherence function (fig. 26) indicates that the identification is valid in the frequency range of 1-7 rad/sec. The poor coherence outside of this frequency range reflects a drop in (open-loop) input power. In the frequency range of validity, the phase comparison is excellent indicating a very accurate model of upper-boost actuator and rotor lags. The roughly parallel shift in the magnitude curves in this frequency range indicates a small gain error in the model. Further indication of model accuracy is obtained from the equivalent system fit of the flight data (1-7 rad/sec):

$$\frac{q}{\delta_{A_\theta}} = \frac{0.283\ e^{-0.0877s}}{(s + 0.610)} \quad \text{rad/sec/in.} \tag{3}$$

The identified equivalent delay of 88 msec matches the rotor and upper-boost delay shown in figure 8, thereby validating these models. For the single degree-of-freedom model of equation (3) the mode is an estimate of the pitch damping M_q. The identified value of 0.610 corresponds very well with the analytical design model value of $M_q = 0.52$ rad/sec (ref. 17). The identified stick sensitivity ($M_{\delta\theta}$) is 13% lower than the design model value, which corresponds to the roughly 1.2 dB magnitude curve shift in figure 25. This error is probably the result of three contributions. One factor is that the design model does not reflect the additional hardware contained in the ADOCS demonstrator as compared with the standard UH-60, thereby increasing the effective pitch inertia and decreasing the pitch sensitivity. A second factor is possible errors in the assumed pitch inertia of the basic UH-60 as contained in the nonlinear simulation program used to determine the design model. Yet a third possible contribution may be the errors in conversion from actuator inches to equivalent pilot stick inches which is done via an analog de-mixing circuit. Nonetheless, the modeling of the open-loop elements seem to be quite acceptable, especially with regard to the model high-frequency delays, a critical aspect in the design as discussed earlier. The reduction in loop gain on the aircraft as opposed to the model will reduce the cross-over frequency thereby

degrading slightly the model following and gust rejection performance, but improving the stability margins.

The comparison of the analytical and identified equivalent system models (eq. (2) and table 11, respectively) is seen to be good (recall that the gain of the analytical model has been normalized). The excellent agreement in overall time delay, along with the open-loop UH-60 agreement, validates the contribution from the remaining digital elements and the ADOCS actuator. The analytical model has a slightly higher natural frequency and damping ratio compared to the flight data which is largely due to the open-loop pitch sensitivity error. Reduction of the loop gain in the analytical model by the 13% discrepancy improves the agreement. The comparison of the bandwidth and phase delay of the analytical model (fig. 11) and the identification result (table 10) is also quite good.

One key finding in reference 8 was that while s-plane (emulation) analysis is useful for evaluating the overall end-to-end response of the digital system, it is not accurate for evaluating the response of the higher frequency elements within the system. Digital filters and actuators respond to the high-frequency sidebands of the zero-order hold, which is not accounted for in the s-plane analysis (see ref. 8). These sidebands create actuator response ripple in the period in between the even sample instants—referred to as intersample ripple. Intersample ripple is important because it causes significant actuator jitter that can cause wear and rate limiting that will go undetected by the control system (which "sees" the measurements only at the even sample instants). This will be most severe for those elements closest to the zero-order hold. In the present system, the ADOCS actuator rate will exhibit the highest degree of intersample response, with reduced intersample response in the ADOCS actuator deflection, and further reduction in the upper-boost actuator responses.

The ADOCS onboard instrumentation system measures actuator responses with a sample rate of 80 Hz, which is roughly three times the sample rate of the AFCS (30 Hz). Also, the instrumentation system contains a 10-Hz filter which will reduce the measured level of intersample response relative to the true motion of the actuator. The (filtered) response of the ADOCS actuator deflection measurement to a longitudinal side-stick input is shown in figure 27a. For illustration purposes, every third symbol is shaded in to roughly distinguish those samples "seen" by the AFCS from the intersample response, however, the measurement system and AFCS are not synchronized, so it is not possible to know exactly at what point the AFCS has been updated. An estimate of the (filtered) actuator rate is obtained from the actuator deflection signal using a central-difference algorithm (fig. 27b). Although this numerical differentiation does introduce some noise into the reconstructed signal, a consistent pattern of actuator ramping during the intersample behavior is very apparent especially toward the end of the 0.5 sec time history. The ripple behavior has a natural period of roughly 3-4 samples of the 80 Hz data, which corresponds to the AFCS update rate. At the end of the record, the intersample ripple has a steady amplitude of 4 in./sec or about 20% of the maximum actuator rate response.

A z-plane analysis of the ADOCS digital control law implementation was not completed. However, the ADOCS digital laws are similar enough to the "practical 4 rad/sec configuration" of the reference 8 case study (for which a comprehensive z-plane analysis was completed) to demonstrate the analytical modeling of the digital characteristics. The digital response of the ADOCS actuator deflection and rate obtained from the 4 rad/sec case study configuration is shown in figure 28 for an input size which has been adjusted to roughly correspond to the flight data case of figure 27. In this figure, the digital response has been passed through a 76 rad/sec low-pass filter which roughly corresponds to the filtering used in the flight data as well. The ratio of the peak actuator rate to deflection (10 in./sec) matches the flight data very well, indicating a satisfactory modeling of the feedback dynamics. The (filtered) ADOCS actuator deflection shows a very small level of intersample ripple, which corresponds to the flight data. The ripple in the

(filtered) actuator rate response is very distinctive, especially at the end of the time history; the ripple amplitude is very close to that seen in the flight data (4 in./sec), thereby substantiating the direct digital analysis procedure.

The true ADOCS actuator response has significantly more intersample ripple, which cannot be seen in the flight data because of the 10 Hz measurement sensor filter. The analytical model response of the ADOCS actuator rate without the sensor filter is shown in fig. 29. A marked increase in the level of intersample ripple is seen for the true ADOCS rate response. Accurate estimates of actuator response and intersample behavior is important for setting specifications of actuator authority, rate limit, wear, and monitoring. Redundancy management systems, which compare the actuator output from parallel channels, will sense unexpectedly large differences in the actuator rate if the system is running asynchronously, as in the ADOCS and many other flight control systems. In the present case, a monitoring rate of at least three times the basic sample rate (equivalent to the instrumentation rate) is needed to accurately monitor the response of the actuators. When the intersample response is excessive, a smoothing filter is often inserted between the zero-order hold and the first actuator. Additional digital analysis methods discussed in reference 8, such as the w-transform and hybrid frequency response, are very useful for evaluating and designing digital control law implementation.

Correlation of Pilot Evaluation and Identification Results with Proposed Handling Qualities Specification

This section correlates pilot evaluation and control response documentation of the ADOCS demonstrator with the proposed military handling qualities specification. The discussion will concentrate on the attitude response characteristics, because control response documentation data for the vertical axis is not currently available.

As discussed earlier, the ADOCS evaluation tasks were limited to moderate amplitude maneuvers (less than about 45° in roll and 25° in pitch) because of safety-of-flight restrictions and in-line monitoring constraints. Since the evaluation was conducted under conditions of unrestricted visibility and without secondary tasks, the applicable paragraphs of the specification are those which refer to the best usable cue environment (UCE = 1) and fully attended operation. Small amplitude specifications given in terms of required minimum bandwidth and phase delay are the same for hover/low speed and forward flight. Similarly, moderate amplitude specifications given in terms of peak angular rate per attitude change are also the same for hover/low speed and forward flight.

The small amplitude boundaries for bandwidth and phase delay applicable to ultra-high gain tasks (target acquisition and tracking) are shown in figure 30, along with the identified ADOCS roll response characteristics for hover. As discussed earlier, slope landings are considered to be ultra-high gain tasks in roll attitude regulation. The identified ADOCS response is seen to plot on the Level 2/Level 3 specification boundary, which is consistent with the numerical handling-qualities ratings for slope landings.. However, the following discussion will argue that the pilot comments explaining the overriding cause of the poor ratings (namely the 1 Hz PIO tendency) indicates that the response should be against a more restrictive phase-delay boundary, and not only against the bandwidth boundary as indicated in figure 30. The roll response identification displays a phase lag of -220° at the 1 Hz pilot crossover frequency noted in the flight records near touchdown. Assuming a pilot neuromuscular lag of 150 msec (typical value), a pilot lead of 140° is necessary to achieve an overall phase margin of 45°. This implies a requirement for two units of pilot lead (since one unit of pilot lead provides a maximum of 90°). As shown in figure 31 (reproduced from ref. 22), two required units of pilot phase lead can be expected to cause severe

handling-qualities degradations, thereby leading to the PIO tendencies displayed in the roll axis. The roll axis equivalent system identification results of table 11 further support the conclusion that command response characteristics based on natural frequency and damping are acceptable (fig. 13), whereas the equivalent time delay (τ_e = 260 msec) will lead to Level 3 handling-qualities in high stress tasks (fig. 4). Time-delay related handling-quality problems were reported for the Bell ARTI heli-copter (ref. 2), which also exhibited equivalent delays exceeding 240 msec. Flight experiments con-ducted by Houston and Horton (ref. 23) using a variable stability PUMA aircraft suggested the need for a phase delay cap of τ_p = 200 msec independent of bandwidth for ultra-high gain tasks. Such a cap would cause the ADOCS response (shown in fig. 30) to be against a phase-delay boundary, which is consistent with the source of the handling-quality problems in slope landings.

Figure 32 is used for all of the roll axis tasks except for the slope landings. All low and medium gain roll axis tasks in both hover and forward flight received solid Level 1 handling-qualities ratings. The normal landing, considered a high gain roll task, received solid Level 2 ratings as a result of 1 Hz PIO problems. Once again the question of a maximum time delay cap is raised based on the hover correlation with the specification as shown in figure 32.

As mentioned earlier, the significant reduction in roll bandwidth for the 80 knot flight condition is due to gain margin limiting resulting from the change from an attitude command to a rate command model along with large time-delays. This command model change occurs automatically as the flight speed increases above 40 knots. The considerable roll and yaw PIO problems in the 60 knots quick stop may be attributable to the (gain-margin limited) bandwidth as indicated in figure 32.

Achievable roll response for moderate amplitude maneuvering are shown in figure 33 to be well within the Level 1 requirements, which is consistent with handling-quality ratings for roll maneuvers such as the return-to-target and level roll reversals.

Running landings are considered to be an ultra-high gain yaw task for the ADOCS aircraft. The correlation shown in figure 34 is consistent with the Level 3 pilot ratings. Further, the associated pilot comments that directional control precision is marginal is consistent with the indication of low bandwidth. As in the roll axis, the low- and medium-gain yaw axis tasks receive Level 1 pilot ratings while high gain tasks such as the lateral escape, 30 knots slalom, and 60 knot quick stop (a high gain yaw task because of coupling) received solid Level 2 ratings. These results are consistent with the correlation of ADOCS response and the specification as shown in figure 35.

Ultra-high gain pitch tasks such as air refueling or aggressive air-to-air tracking in the vertical plane were not completed during the ADOCS evaluation. Therefore, no correlation with the proposed ultra-high gain pitch boundary is possible. High-gain pure pitch tasks such as low-level contour flying were not completed in the displacement collective evaluation reported in this paper. Low- and medium-gain pitch tasks as with the roll and yaw axes, received consistent Level 1 ratings. These pitch ratings are consistent with the proposed small amplitude specification (fig. 36). However, pilot comments (table 8) concerning longitudinal control sluggishness during the 30-knot slalom (a high-gain predominantly roll/yaw task) suggest that the pitch bandwidth boundary should perhaps be raised. Correlation of pitch characteristics for moderate amplitude maneuvering is shown in figure 37. The correlation is consistent with Level 1 handling qualities for moderate amplitude pitch tasks such as the initiation of the dash.

Summarizing the correlation of the ADOCS handling qualities results for the displacement collective with the proposed handling qualities specification indicates: (1) Bandwidth specifications for ultra-high and high gain tasks are consistent with the pilot evaluation. (2) Phase delay restrictions are too lenient. A

phase delay cap of 200 msec proposed by previous researchers is supported by the ADOCS flight experiments.

CONCLUSIONS

1. High-bandwidth handling-qualities requirements for advanced combat rotorcraft are achievable with current technology, but require careful allocation and accounting of time delays and high-frequency dynamics in the design process.

2. An analytical study indicates that desirable control response characteristics based on equivalent damping and frequency are achievable with the ADOCS explicit model-following structure. Excessive equivalent time delays (exceeding 240 msec in all axes) in the ADOCS are mostly due to the rotor, stick filter, and actuator dynamics.

3. Piloted evaluation of the ADOCS 3+1 (displacement collective) AFCS configuration indicates handling-qualities that are desirable (Level 1) or marginally desirable (borderline Level 1/2) for low and moderate gain tasks. Handling-qualities are adequate (Level 2) for high gain tasks, and are inadequate (Level 3) for ultra-high gain tasks such as slope and running landings. The primary cause of ADOCS handling-qualities deficiencies is considered to be excessive equivalent time-delays.

4. Analytical models based on emulation (s-plane) techniques compare favorably with flight-extracted frequency-domain characteristics of the overall (end-to-end) ADOCS responses. Direct digital analysis procedures are shown to be necessary to characterize the intersample behavior of the actuator rate response.

5. Correlation of the piloted evaluation results with the proposed handling-qualities specification indicates generally good agreement for the bandwidth boundaries, but suggests the need for more stringent limits on allowable phase delay.

REFERENCES

1. Glusman, S. I.; Dabundo, C.; Landis, K. H.: Evaluation of ADOCS Demonstrator Handling Qualities. 43rd Annual National Forum of the American Helicopter Society, Washington, DC, May 1987.

2. Hendrick, R.; Ramohalli, G.; Yanke, D.; Fortenbaugh, R.; and Freeman, T.: Advanced Flight Control Development for Single-Pilot Attack Helicopters. 42nd Annual Forum of the American Helicopter Society, Washington, DC, June 1986.

3. Gupta, B. P.; Barnes, B. B.; Dockter, G.; Hodge, R.; and Morse, C.: Design Development and Flight Evaluation of an Advanced Digital Flight Control System. 43rd Annual National Forum of the American Helicopter Society, Washington, DC, May 1987.

4. Hoh, R. H.; Mitchell, D. G.; Aponso, B. L.; Key, D. L.; and Blanken, C. L.: Proposed Specification for Handling Qualities of Military Rotorcraft. Vol. 1—Requirements. USAAVSCOM Tech Report 87-A-4. Draft dated May 1988.

5. Hilbert, K. B.; Lebacqz, J. V.; and Hindson, W. S.: Flight Investigation of a Model-Following Control System for Rotorcraft. AIAA 3rd Flight Testing Conference, Las Vegas, NE, April 1986.

6. Holdridge, R. D.; Hindson, W. S.; and Bryson, A. E.: LQG-Design and Flight-Test of a Velocity-Command System for a Helicopter. AIAA CP, AIAA Guidance, Navigation, and Control Conference, Snowmass, CO, August 1985.

7. Chen, R. T. N.; and Hindson, W. S.: Influence of Higher-Order Dynamics on Helicopter Flight-Control System Bandwidth. AIAA J. of Guidance, Control and Dynamics, vol. 9, no. 2, March/April 1986, pp. 190-197.

8. Tischler, M. B.: Digital Control of Highly Augmented Combat Rotorcraft. NASA TM-88346, ARMY TR 87-A-5, May 1987.

9. Tischler, M. B.; Fletcher, J. W.; Dickman, V. L.; Williams, R. A.; and Cason, R. W.: Demonstration of Frequency-Sweep Test Technique Using a Bell-214-ST Helicopter, NASA TM-89422, ARMY TM 87-A-1, April 1987.

10. Heffley, R. K.; Bourne, S. M.; Curtiss, H. C., Jr.; Hindson, W. S.; and Hess, R. A.: Study of Helicopter Roll Control Effectiveness Criteria. NASA CR-177404, USAAVSCOM TR 85-A-5, April 1986.

11. Mitchell, D. G.; Hoh, R. H.; and Morgan, J. M.: A Flight Investigation of Helicopter Low-Speed Response Requirements. J. Guidance, Control, and Dynamics (forthcoming).

12. Aiken, E. W.: Simulator Investigations of Various Side-Stick Controller/Stability and Control Augmentation Systems for Helicopter Terrain Flight. AIAA Paper 82-1522, 1983.

13. Landis, K. H.; Dunford, P. J.; Aiken, E. W.; and Hilbert, K. B.: Simulator Investigations of Side-Stick Controller/Stability and Control Augmentation Systems for Helicopter Visual Flight. J. of American Helicopter Society, April 1985, pp. 3-13.

14. Tischler, M. B.: Assessment of Digital Flight Control for Advanced Combat Rotorcraft. American Helicopter Society National Specialists Meeting on Flight Controls and Avionics, Cherry Hill, NJ, October 1987.

15. Smith, E. E.; and Sarrafan, S. K.: Effect of Time Delay on Flying Qualities: An Update. AIAA J. of Guidance, Control, and Dynamics, vol. 9, no. 5, 1986, pp. 578-584.

16. Glusman, Steven I.; Landis, Kenneth H.; and Dabundao, Charles: Handling Qualities Evaluation of the ADOCS Primary Flight Control System. 42nd Annual Forum of the American Helicopter Society, Washington, DC, June 1986.

17. Landis, Kenneth H.; and Glusman, Steven I.: Literature Review and Preliminary Analysis. Development of ADOCS Controllers and Control Laws, vol. 2, TR-84-A-7, USAAVSCOM, 1985. (Also NASA CR-177339, 1985.)

18. Hoh, Roger H.; and Ashkenas, Irving L.: Development of VTOL Flying Qualities Criteria for Low Speed and Hover. TR-1116-1, Systems Technology, Inc., Hawthorne, CA, 1979.

19. Hoh, Roger H.; and Mitchell, David G.: Proposed Revisions to MIL-F-8330 V/STOL Flying Qualities Specification. NADC-82146-60, January 1986.

20. Cooper, G. E.; and Harper, R. P.: The Use of Pilot Rating in the Evaluation of Aircraft Handling Qualities. NASA TN D-5153, April 1969.

21. Tischler, M. B.: Frequency-Response Identification of XV-15 Tilt-Rotor Aircraft Dynamics. NASA TM-89428, ARMY TM 87-A-2, May 1987.

22. Ashkenas, I. L.: Pilot Modeling Applications. AGARD-LS-157, Advances in Flying Qualities.

23. Houston, S. S.; and Horton, R. I.: The Identification of Reduced Order Models of Helicopter Behaviour for Handling Qualities Studies. Presented at the Thirteenth European Rotorcraft Forum, Arles, France, 8-11 September 1987.

TABLE 1.– ADOCS AFCS FEEDBACK GAINS IN HOVER

Feedback signal	Simulation	Initial Flight value	Current Flight value	Total % change
Pitch rate (in./rad/sec)	16.0	6.4	6.8	-58
Pitch attitude (in./rad)	34.0	13.6	10.4	-69
Roll rate (in./rad/sec)	6.0	2.4	1.3	-78
Roll attitude (in./rad)	20.0	8.0	8.4	-58
Yaw rate (in./rad/sec)	7.2	3.2	4.0	-44
Heading (in./rad)	7.7	7.6	7.6	-1
			Average:	-51

TABLE 2.– SUMMARY OF COMMAND MODELS FOR ANGULAR RESPONSES

Axis	Hover	V > 40 knots
pitch, θ_m/θ_c	$\frac{4(s + 0.2)}{s(s + 2)(s + 2)}$	same as hover
roll, ϕ_m/ϕ_c	$\frac{6.25(s + 0.33)}{s(s + 2.5)(s + 2.5)}$	$\frac{5.08}{s(s + 5.08)}$
yaw, ψ_m/ψ_c	$\frac{2}{s(s + 2)}$	same as hover

TABLE 3.– SUMMARY OF EQUIVALENT TIME DELAYS IN ADOCS FLIGHT CONFIGURATION PITCH CHANNEL

Element	Delay (msec)	% of total
Rotor	66	30
Actuators	31	14
Zero-order hold	17	8
Computations	22	10
Notch filter	11	5
Stick filter	59	26
Stick sampling skew	17	8
Total delay	223 msec	

TABLE 4.– FLIGHT TEST HOURS FOR AFCS EVALUATION

	Controller	Number of Flights	AFDD	Boeing
3+1	(Displacement collective)			
	Frequency sweeps	2		4:15 hr
	Handling qualities	6	11:12 hr	
3+1	(Force collective)			
	Frequency sweeps	2		1:48 hr
	Handling qualities	3	5:44 hr	
4+0				
	Handling qualities	1 aborted		
	Totals	14	16:56 hr	6:03 hr

TABLE 5.– ADOCS COMMAND/STABILIZATION MODES
COLLECTIVE DISPLACEMENT
Core AFCS Displacement

Mode	Less than 40 knots	Greater than 40 knots
Longitudinal	Attitude/attitude	Attitude/airspeed hold
Lateral	Attitude/attitude If $p < 1°$/sec and $\phi < 3°$	Rate/attitude If $p < 1°$/sec
Vertical	Direct control of collective pitch angle	
Directional	Acceleration/rate	Turn coordination on lateral stick above 50 knots
	Core AFCS plug heading hold	
Directional inflight	Rate/attitude Full time head hold < 40 knots. Synchronized heading on lateral stick > 40 knots	Rate/attitude Turn coordination on lateral stick > 50 knots
	Heading remains synchronized regardless of airspeed if lateral or directional stick out of detent or $p > 3°$/sec or $\phi > 3°$ or $r > 1°$/sec	
Taxi	Rate/heading hold	

TABLE 6.– LOW-GAIN TASKS

Task	Focus of pilot effort	HQRs		
		Ave	Range	Samples
Wings level cruise	Directional out of trim and slight roll attitude offset at bank angle <3°	3	3	Many
Turning flight	Excellent attitude and directional trim hold	2	1-2	Many
Precision hover/translation	Excellent attitude stability	2	1-3	4
360° hover turn	Slightly jerky yaw response with heading hold	2.5	2-3	2
Transition to forward flight/ dash maneuver	Slightly sluggish in pitch	3	3	Many

TABLE 7.– MEDIUM-GAIN TASKS

Task	Focus of pilot effort	HQRs		
		Ave	Range	Samples
Hover circle	Steppy yaw response with heading hold engaged. Yaw response improved without heading hold	3	2.5-4	3
Approach to hover	Anticipation of power requirements at hover	3	2.5-3	3
Bob ups	Position hold without hover mode engaged HQR 3. HQR 2 with hover and radar altitude hold	2.5	2-3	3
Sideward flight	Excellent heading hold. Good lateral control	3	3	3
Directional target switching	Increased pointing accuracy with heading hold engaged	3/4	3-4	2
180° return to target	Excellent roll and pitch attitude control	3	3	3
Roll reversal, forward flight	Some overshoot in aggressive maneuvering	3	3	1
15 knot slalom	Somewhat sluggish longitudinally, steppy directionally with heading hold, better without	3/4	3-4	3
Lateral jinks	Good heading hold. Some overshoot in roll on input and recovery	3	3	1

TABLE 8.– HIGH-GAIN TASKS

Task	Focus of pilot effort	HQRs		
		Ave	Range	Samples
Lateral escape	Directional coordination in lateral to longitudinal transition HQR = 6 with heading hold, 4-4.5 without	4.5	4-6	4
30 knot slalom	Sluggish longitudinally with high workload for directional coordination. Much smoother directionally without heading hold. Lateral oscillation with velocity stabilization selected	5	4.5-6	6
Normal landing				
Touchdown	Excellent up to touchdown, where 1 Hz lateral observed	4.5	4-5	Many
Lift off	Much harder to predict proper lateral control position for lift off	One HQR worse than landing		
60 knot quickstop	Right yaw slice in flare. Considerable roll PIO	5	4-6	3
Ground taxi	Required directional control precision not available	5	3-9	Many

TABLE 9.– ULTRA-HIGH GAIN TASKS

Task	Focus of pilot effort	HQRs		
		Ave	Range	Samples
Lateral slope operations				
Landing	Impossible with right wheel upslope. Consistent right yaw at touchdown followed by monitor trip. With left gear upslope, lateral 1 Hz consistent throughout landing	5	4-9	10
Lift-off	Difficult to predict lateral and directional control requirements in lift-off	One HQR worse than landing task		
Running landing				
Nose high	Impossible because of ADOCS monitor trips at tail wheel touchdown	---	---	3
Level attitude	Directional control precision marginal	8	8	3

TABLE 10.– SUMMARY OF IDENTIFIED BANDWIDTH AND PHASE DELAY VALUES

Hover				80 knots			
Axis	ω_{BW_g}, rad/sec	ω_{BW_p}, rad/sec	τ_p, sec	Axis	ω_{BW_g}, rad/sec	ω_{BW_p}, rad/sec	τ_p, sec
Pitch	<u>2.10</u>	2.27	0.202	Pitch	<u>1.84</u>	2.40	0.181
Roll	<u>2.33</u>	2.38	0.181	Roll	<u>0.94</u>	1.53	0.175
Yaw (pedals) (heading hold)	1.70	<u>1.33</u>	0.138	Yaw (pedals) (heading hold)	<u>1.68</u>	1.77	0.206

Note: Bandwidth frequency, ω_{BW} = lesser of ω_{BW_g} and ω_{BW_p} is underlined

TABLE 11.– SUMMARY OF IDENTIFIED TRANSFER–FUNCTION MODELS

Hover		80 knots	
Model	Frequency range, rad/sec	Model	Frequency range, rad/sec
$\frac{\theta}{\delta_{LON}} = \frac{-0.876(s + 0.229)e^{-0.238s}}{s[0.539,\ 1.82]}$	0.209–6.75	$\frac{\theta}{\delta_{LON}} = \frac{-0.894(s + 0.131)e^{-0.254s}}{s[1.09,\ 1.63]}$	0.209–8.0
$\frac{\phi}{\delta_{LAT}} = \frac{3.10(s + 0.234)e^{-0.260s}}{s[1.39,\ 2.28]}$	0.209–9.03	$\frac{\phi}{\delta_{LAT}} = \frac{1.17\ e^{-0.239s}}{s(s + 2.65)}$	0.209–12.0
$\frac{\psi}{\delta_{PED}} = \frac{1.15\ e^{-0.224s}}{s(s + 2.76)}$ (heading hold)	0.209–6.00	$\frac{\psi}{\delta_{PED}} = \frac{0.715\ e^{-0.327s}}{s(s + 5.12)}$ (heading hold)	0.8–6.00

θ, ϕ, ψ in degrees

$\delta_{LON}, \delta_{LAT}, \delta_{PED}$ in percent

Figure 1.– Advanced Digital Optical Control System (ADOCS) demonstrator.

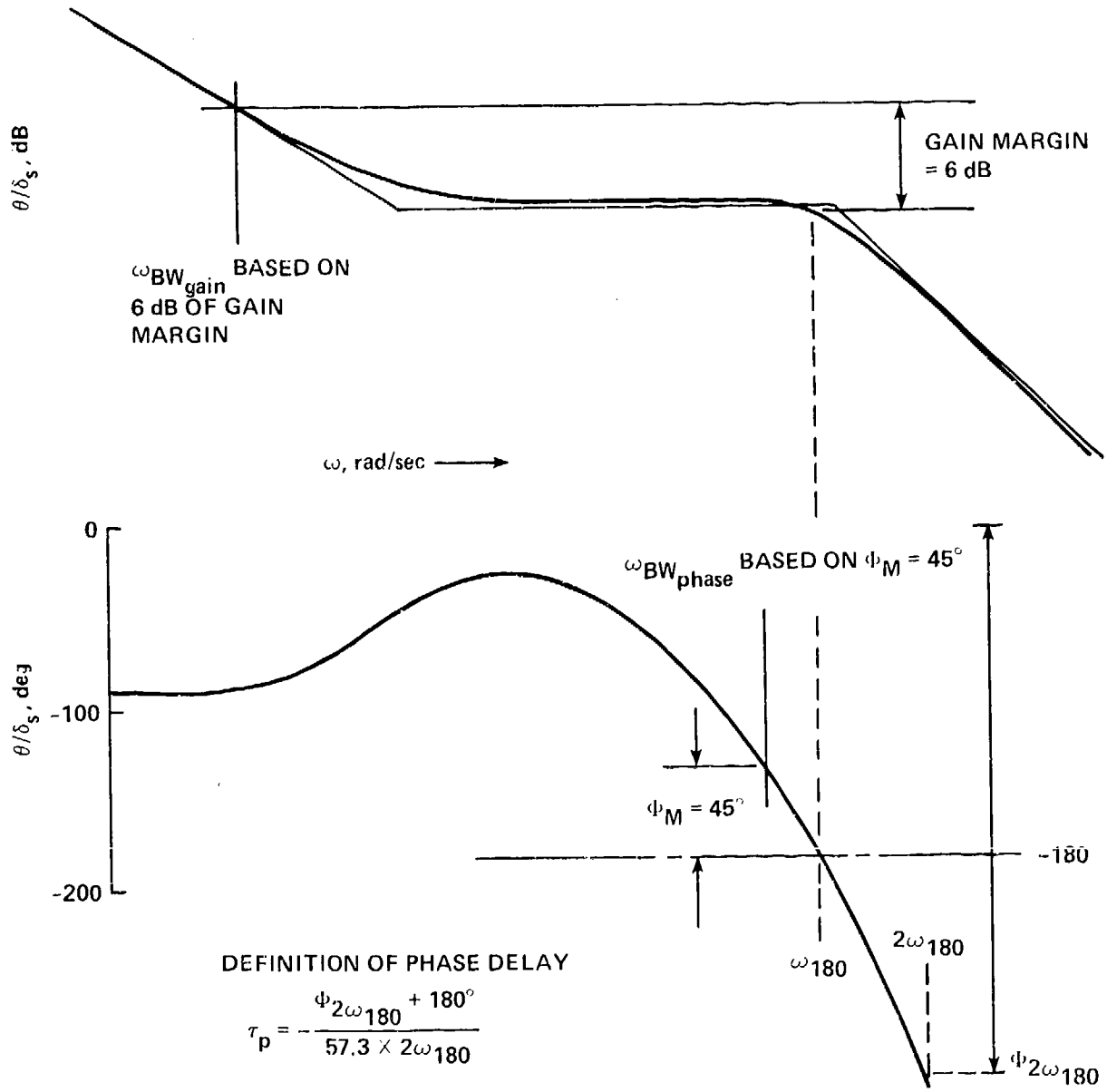

Figure 2.– Definition of bandwidth (ω_{BW}) and phase delay (τ_p). For attitude response type, $\omega_{BW} = \omega_{BW_{phase}}$. For rate response type, ω_{BW} is the lesser of $\omega_{BW_{phase}}$ and $\omega_{BW_{gain}}$.

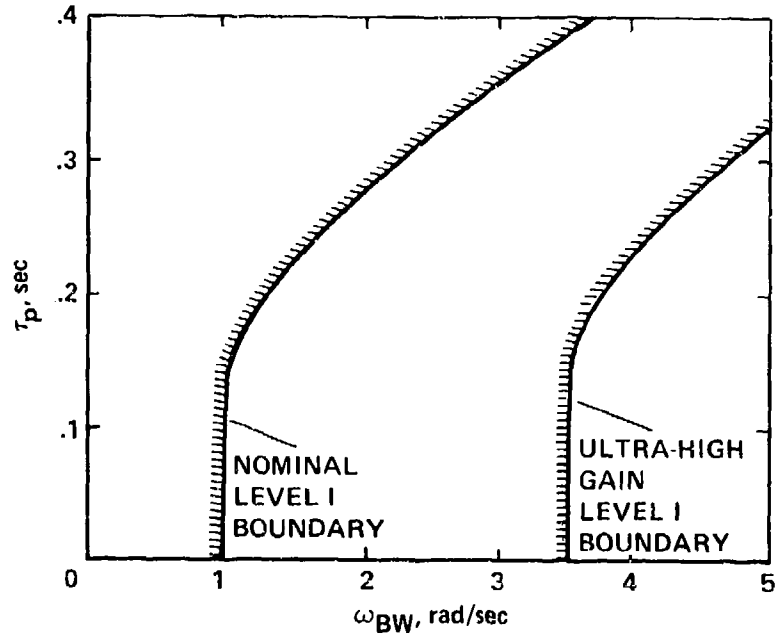

Figure 3.– Level 1 small-amplitude pitch requirements for minimum and maximum gain tasks.

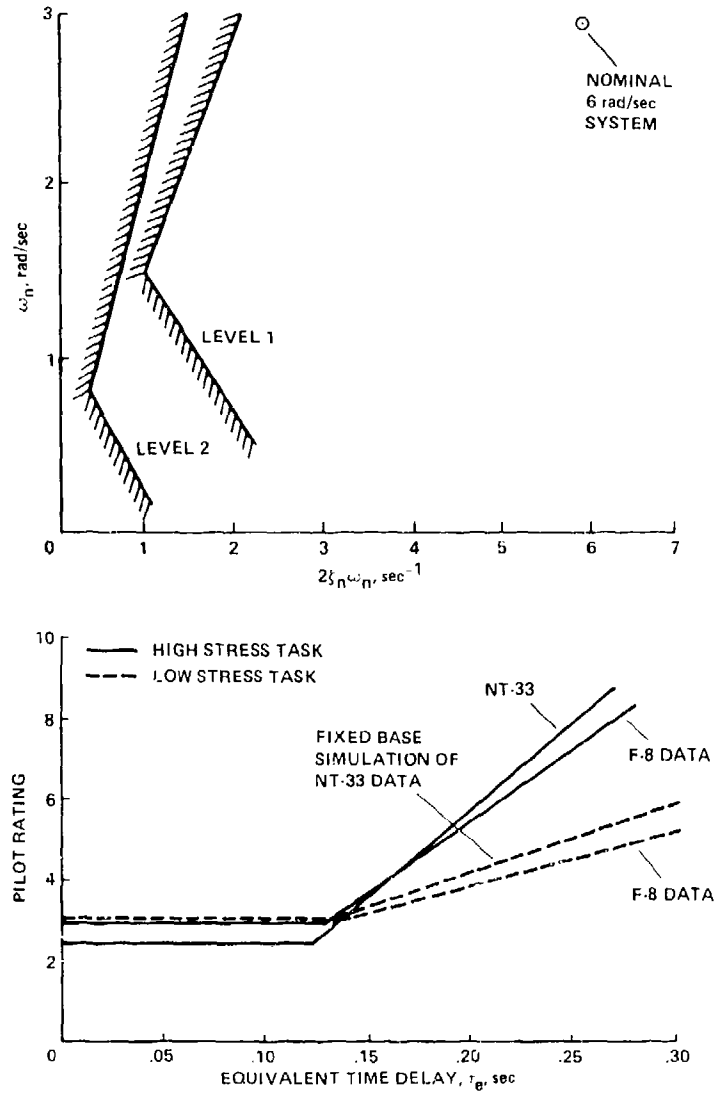

Figure 4.– Effect of time delay on pilot handling-qualities for low- and high-stress tasks, from reference 15.

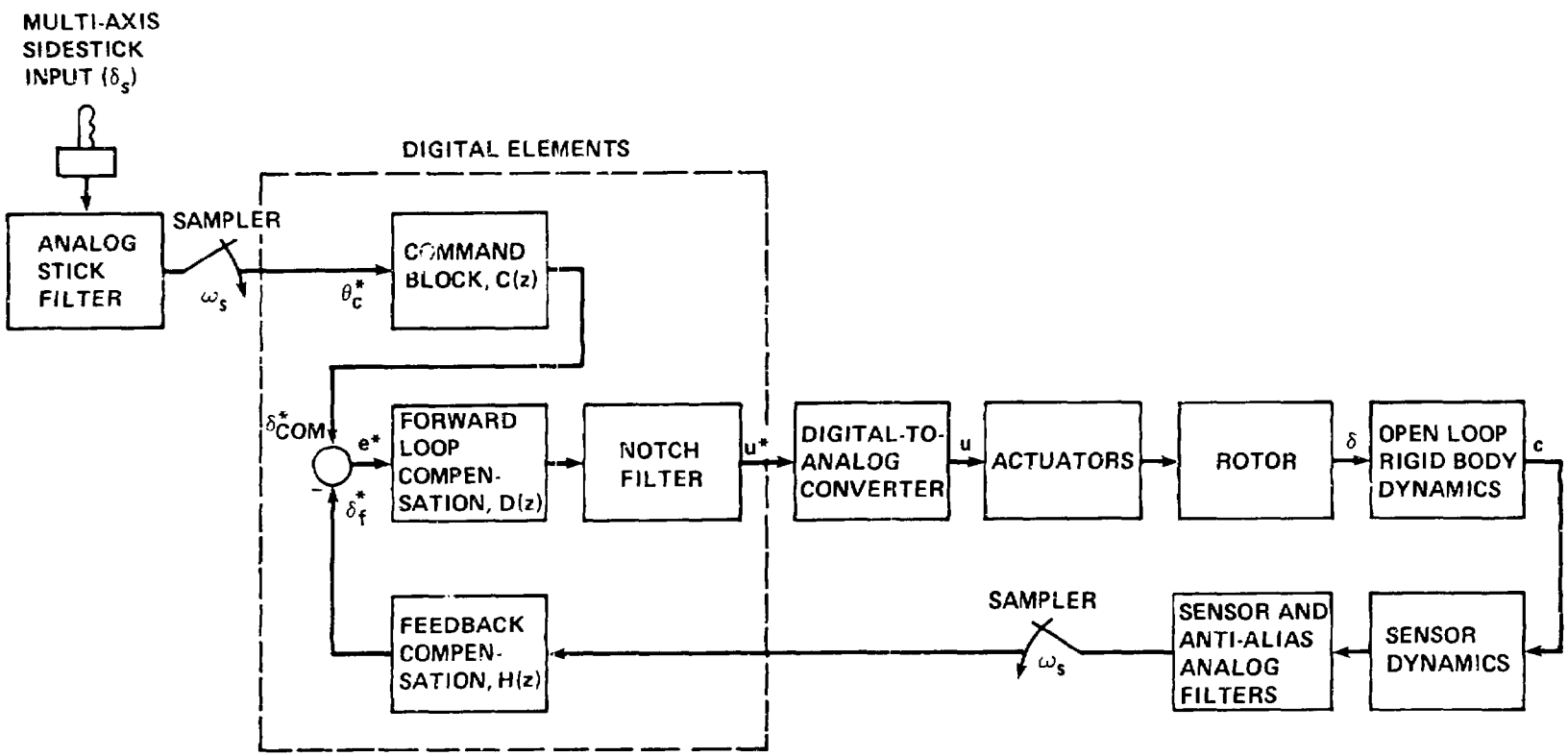

Figure 5.– Generic high-bandwidth analog flight-control system.

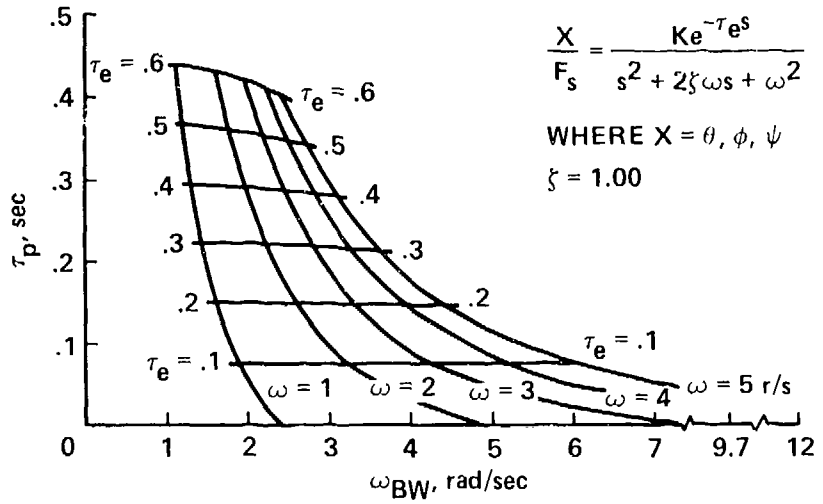

Figure 6.– Cross-plot of natural frequency, bandwidth, equivalent time-delay, and phase delay for a second-order attitude response type.

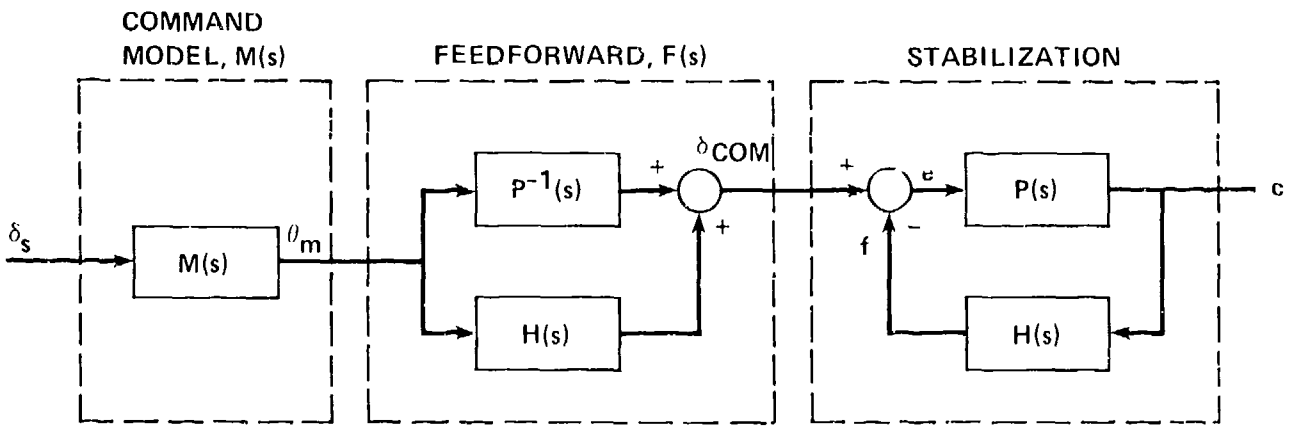

Figure 7.– ADOCS generic model-following concept.

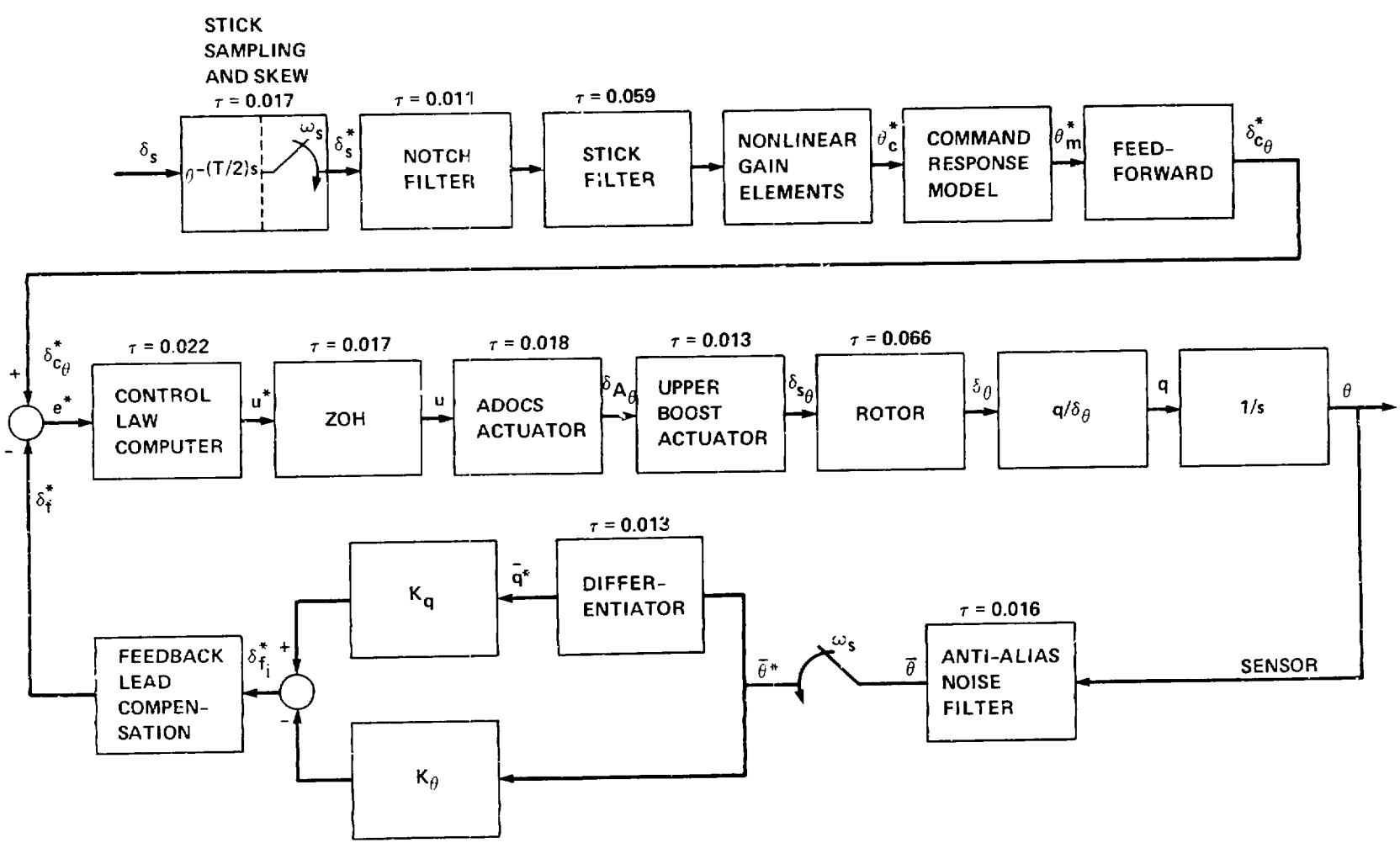

Figure 8.– Simplified schematic of ADOCS pitch channel in hover; effective time delay for high-frequency dynamics are indicated in figure.

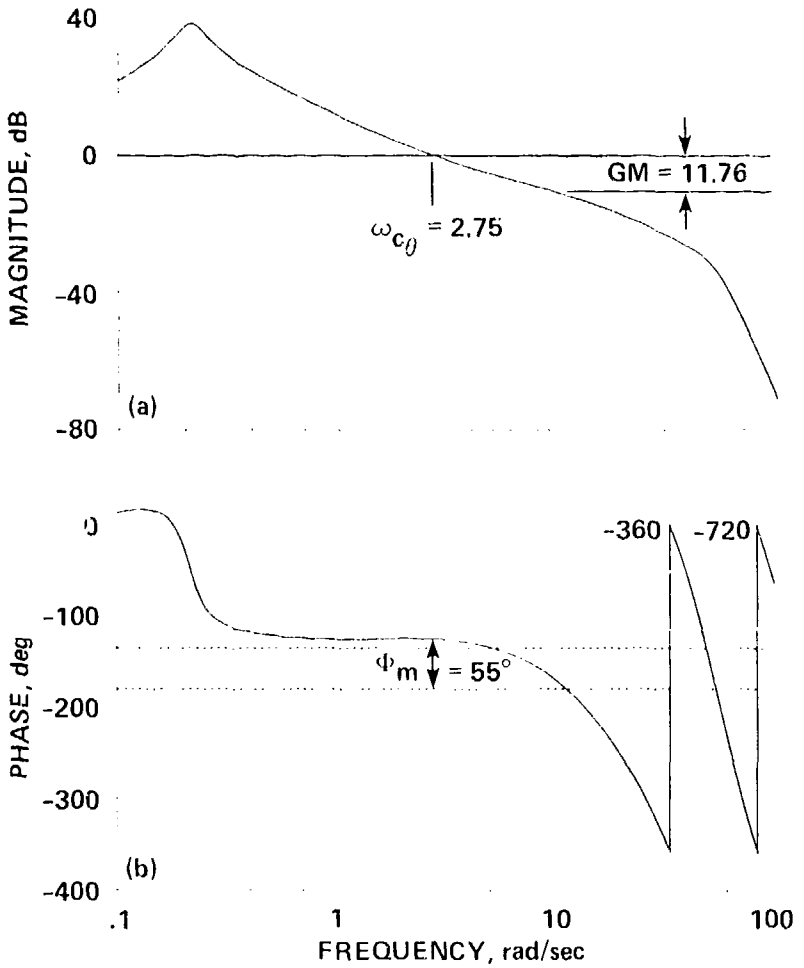

Figure 9.– Equalized open-loop frequency-response of ADOCS pitch channel stabilization loop; (a) magnitude, (b) phase.

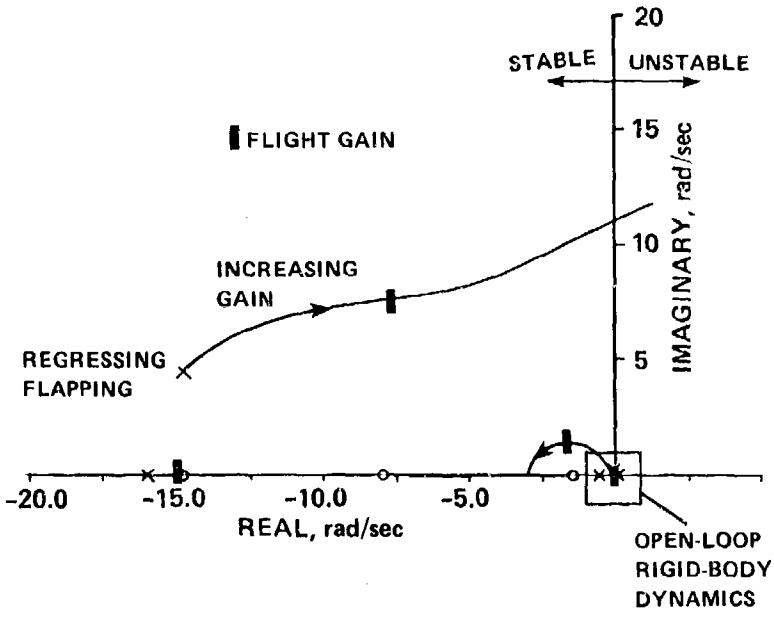

Figure 10.– Pitch channel root locus for stabilization loop versus loop gain.

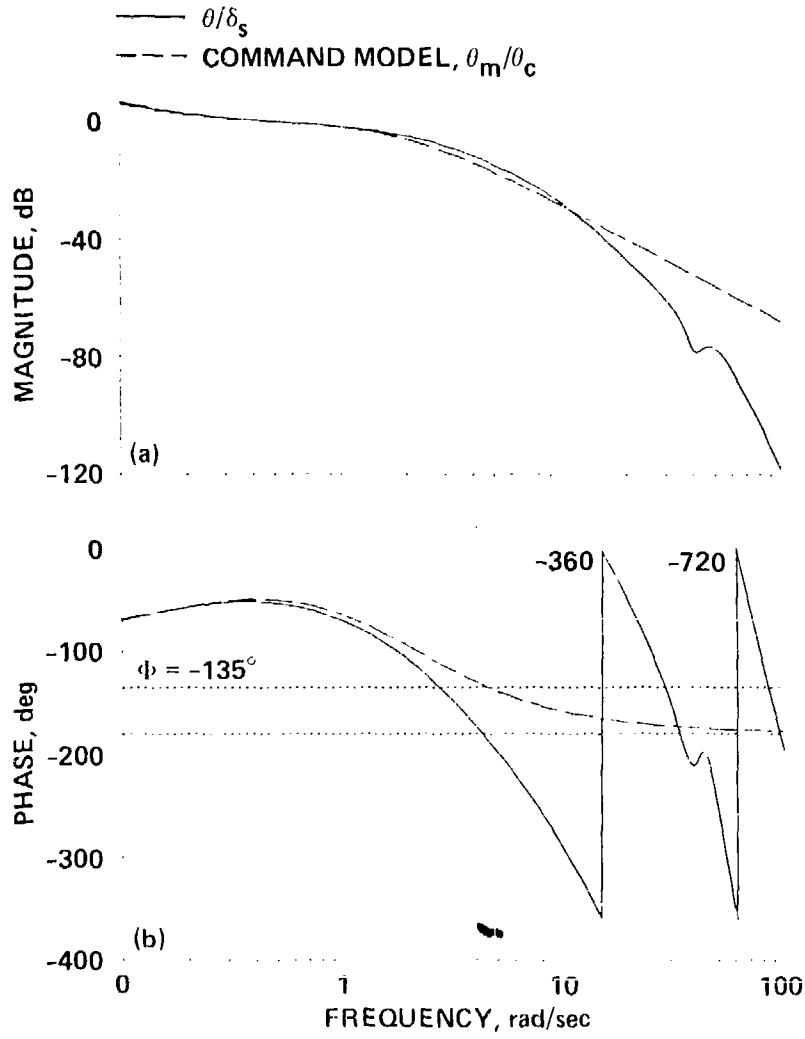

Figure 11.– Overall frequency-response of the pitch system (θ/δ_s) compared with the command model (θ_m/θ_c); (a) magnitude; (b) phase.

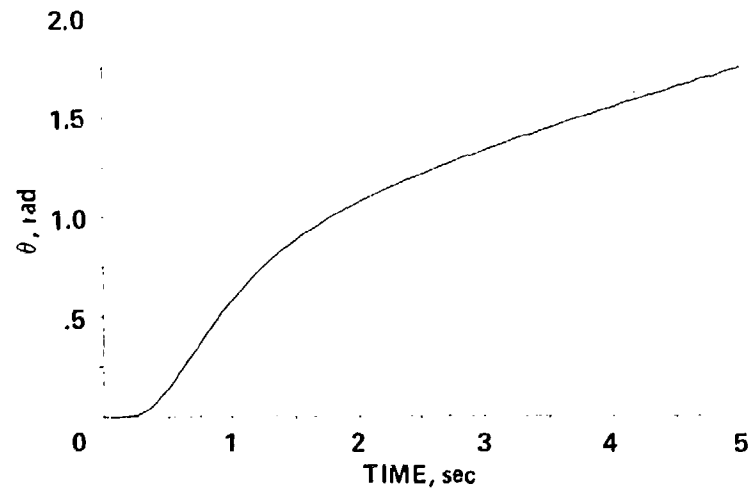

Figure 12.– Normalized pitch attitude response to a step input in hover.

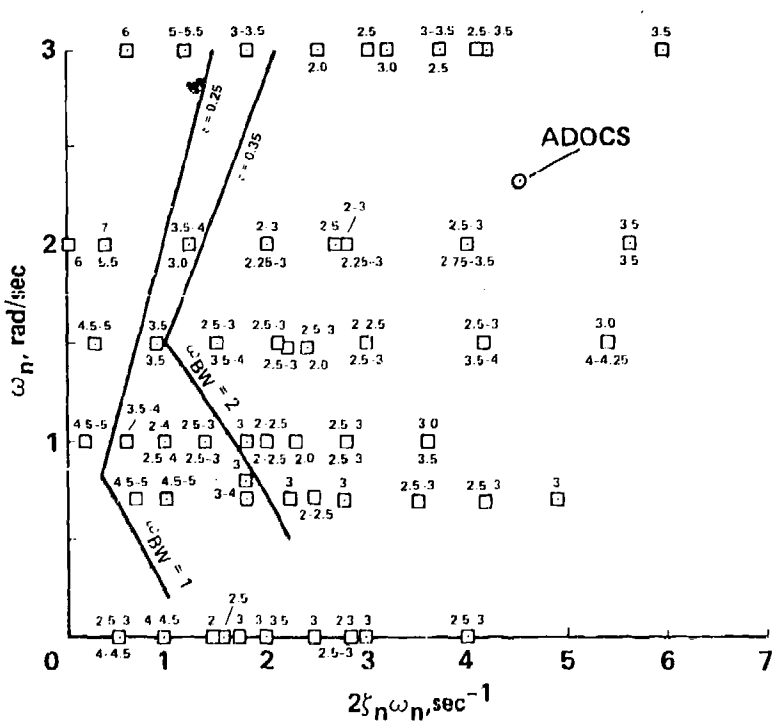

Figure 13.– Handling-qualities data from reference 18 and lines of constant bandwidth.

Figure 14.– ADOCS evaluation pilot station with 3+1c configuration.

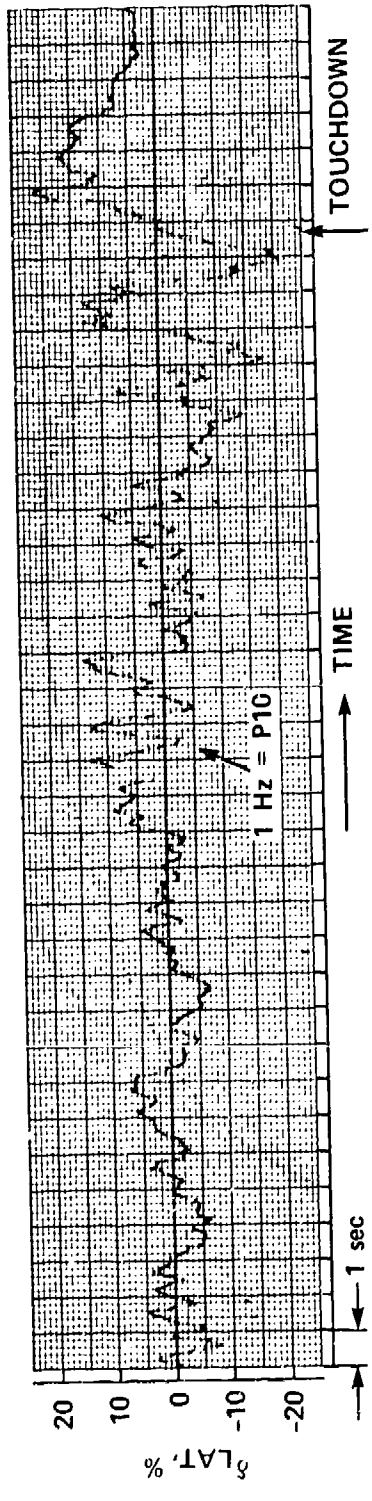

Figure 15.– Flight record of vertical landing; note persistent 1 Hz oscillations.

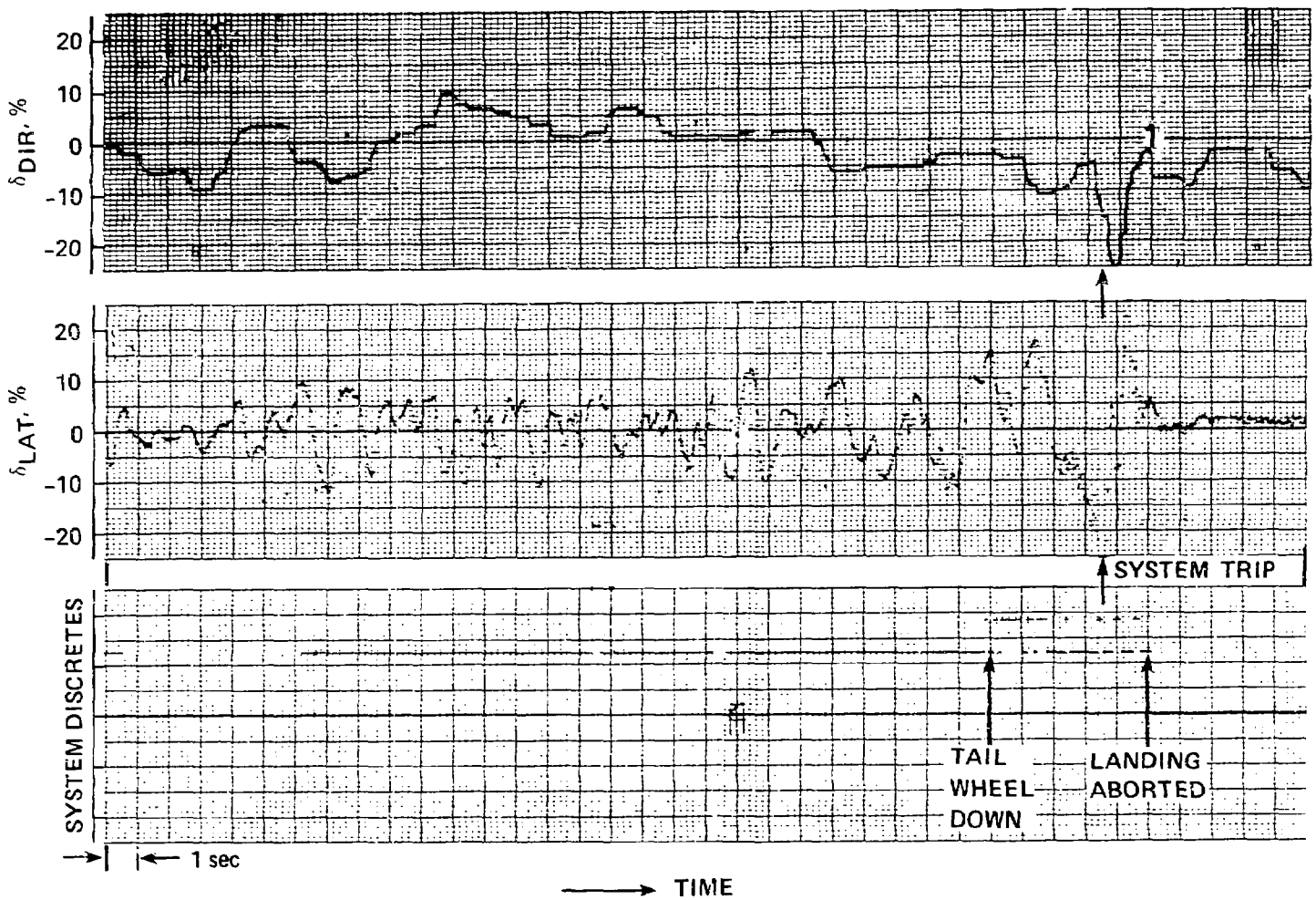

Figure 16.– Flight record of aborted slope landing with left wheel downslope.

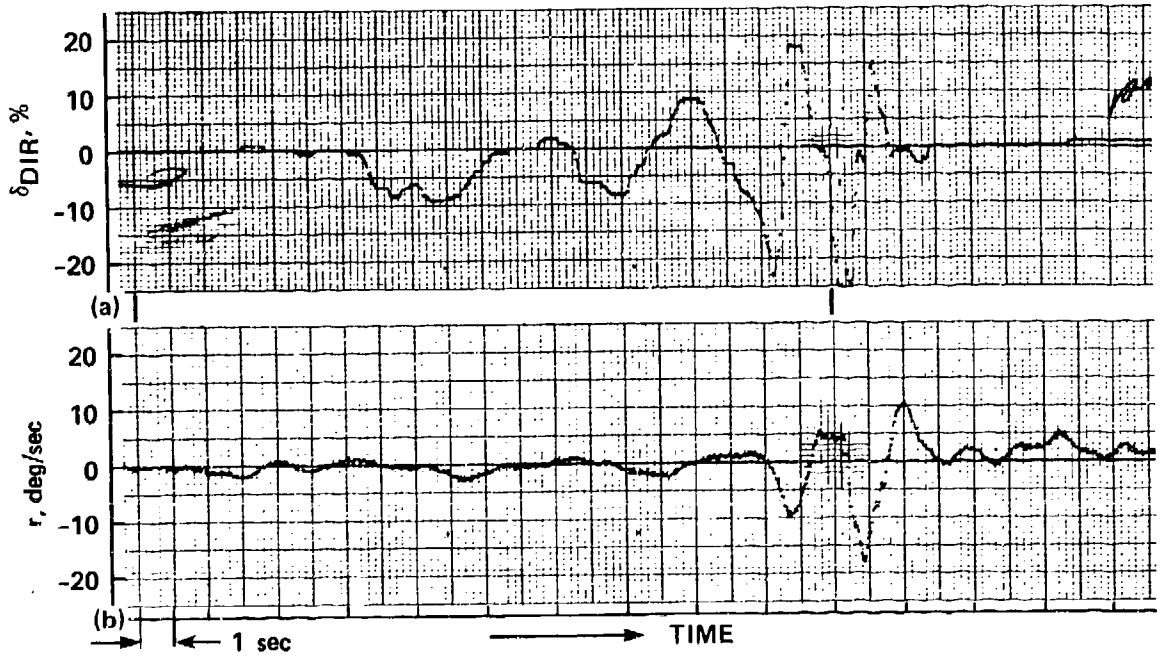

Figure 17.– Flight record of running landing; (a) pilot directional input, (b) yaw rate response.

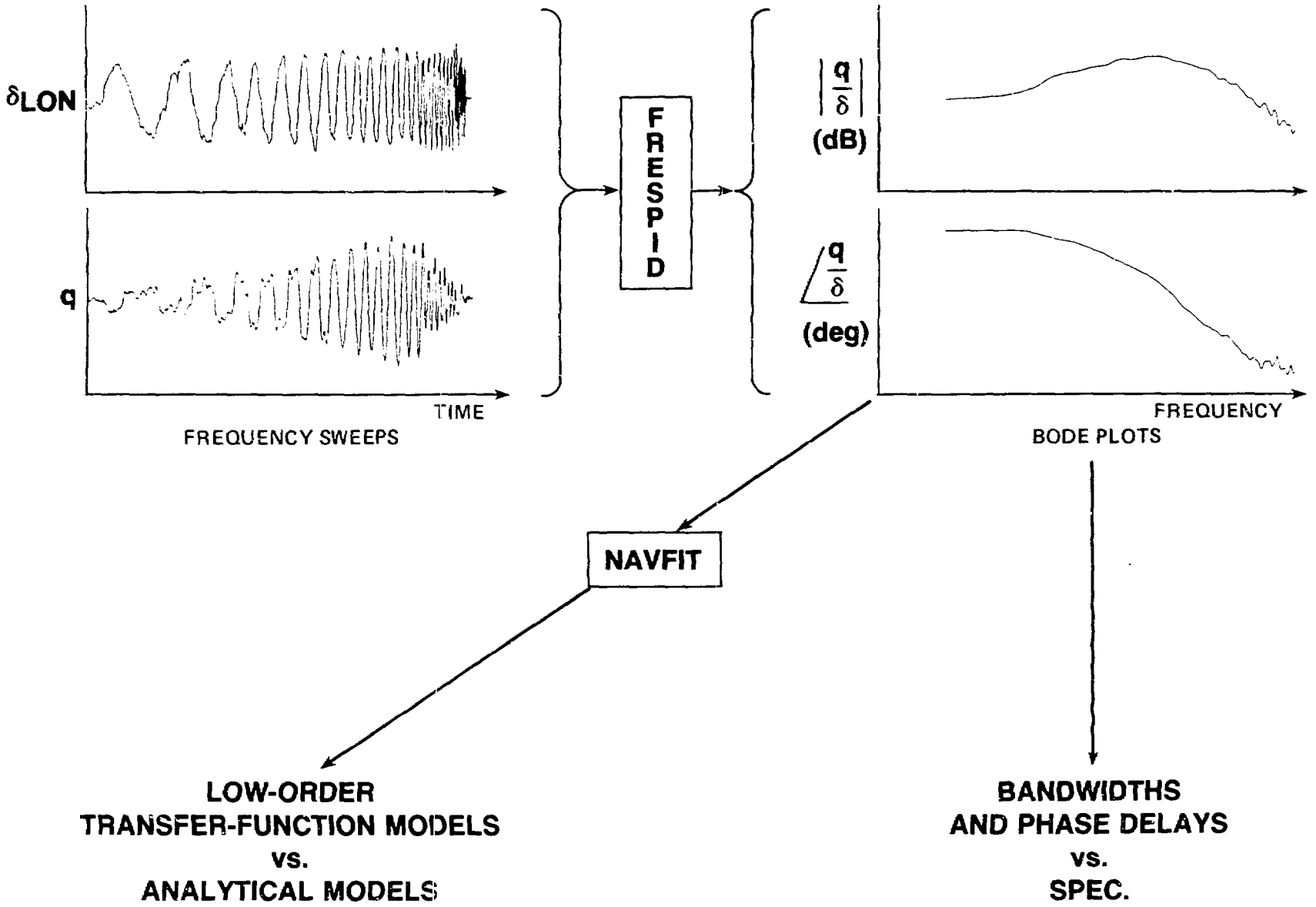

Figure 18.– Frequency-domain system identification procedures.

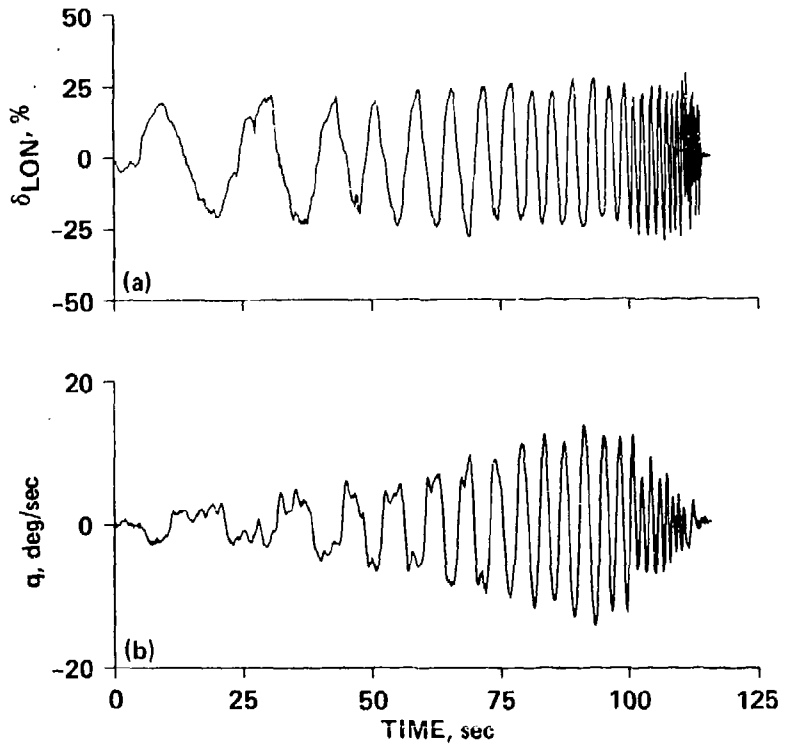

Figure 19.– Longitudinal side-stick frequency-sweep in hover; (a) pilot input, (b) pitch rate.

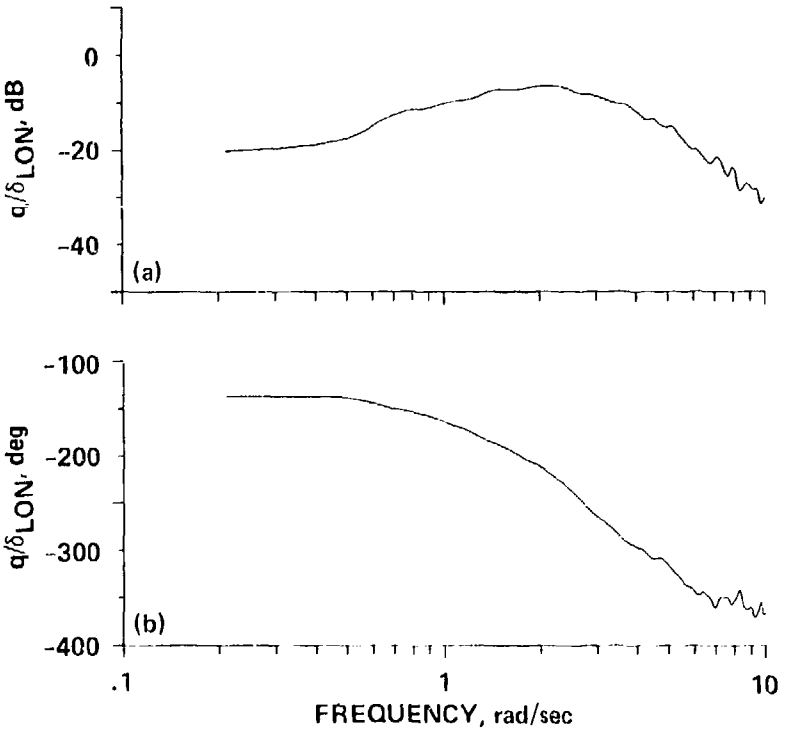

Figure 20.– Identification of pitch rate response to longitudinal side-stick for six concatenated sweeps in hover.

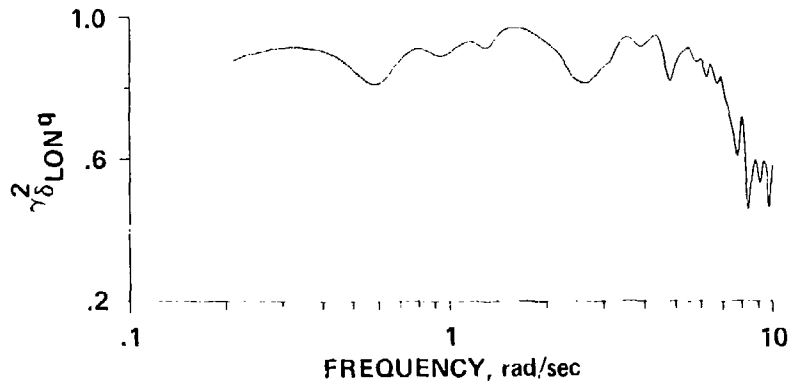

Figure 21.– Coherence for pitch rate response identification.

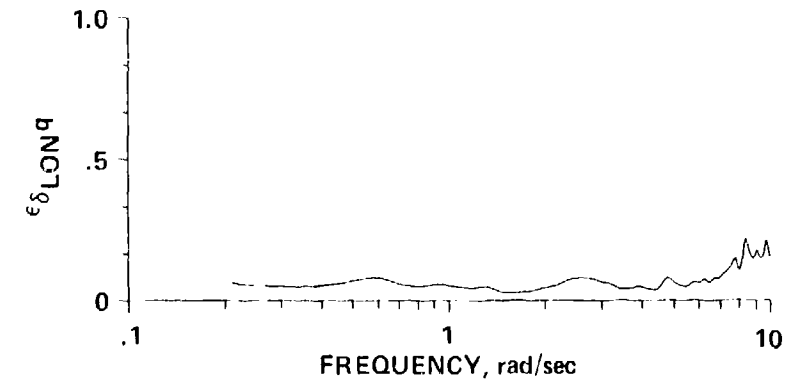

Figure 22.– Normalized random error for pitch rate response identification.

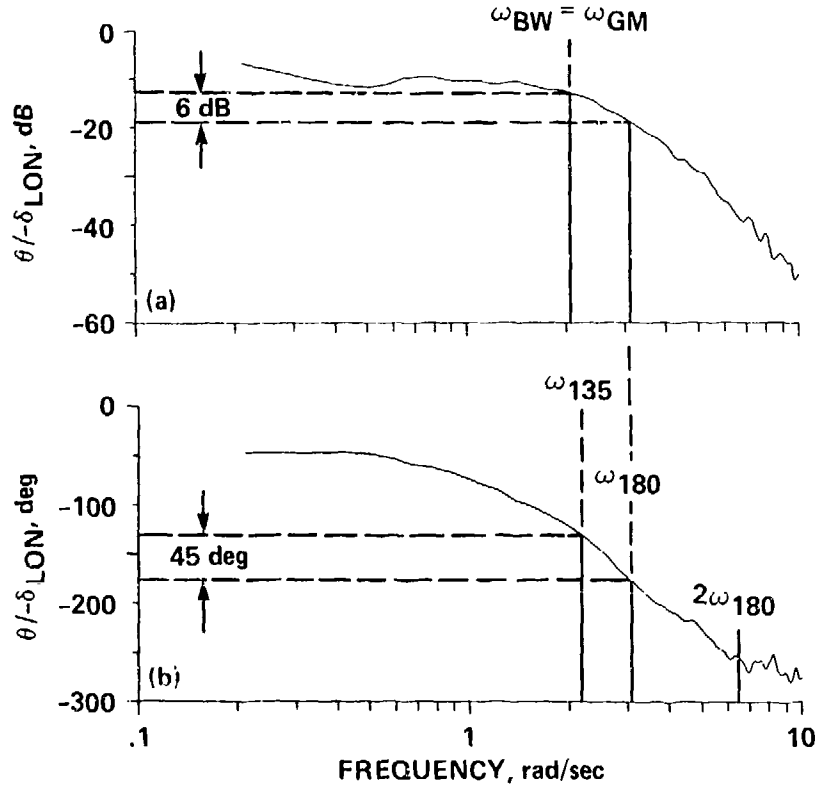

Figure 23.– Determination of bandwidth and phase delay from pitch attitude response in hover.

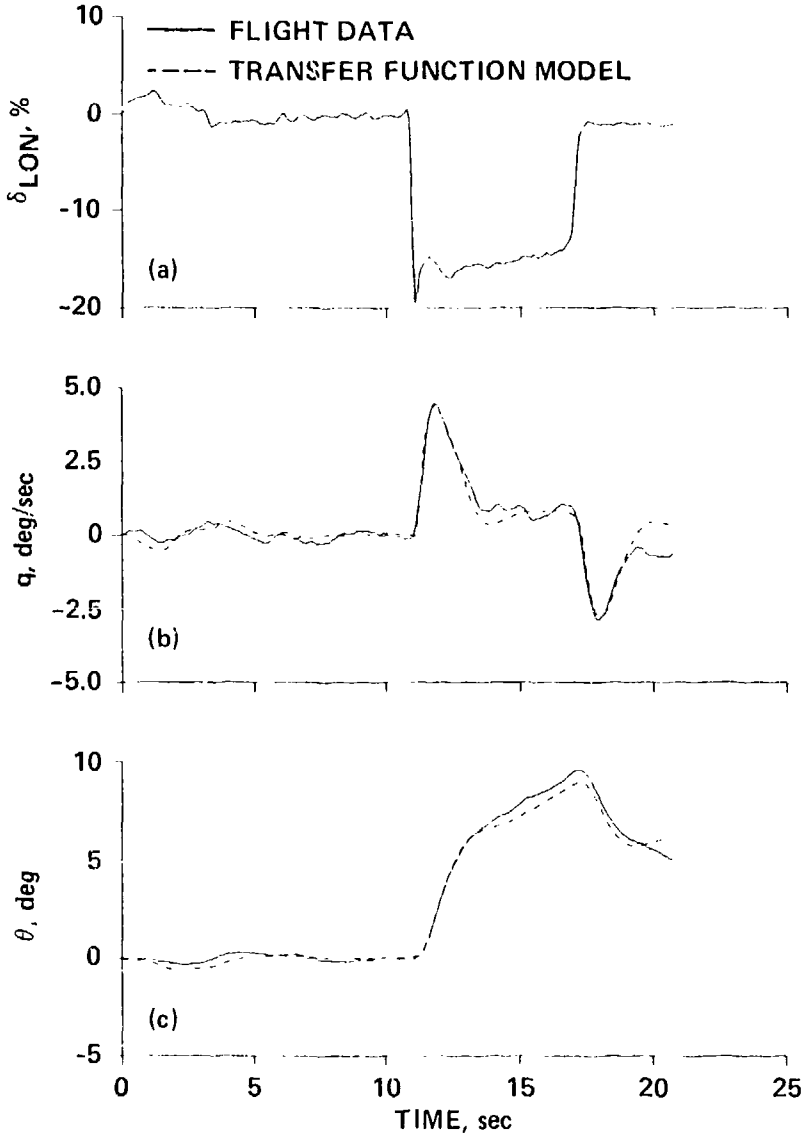

Figure 24.– Verification of identified pitch response transfer-function model. (a) pilot input, (b) pitch rate, (c) pitch attitude.

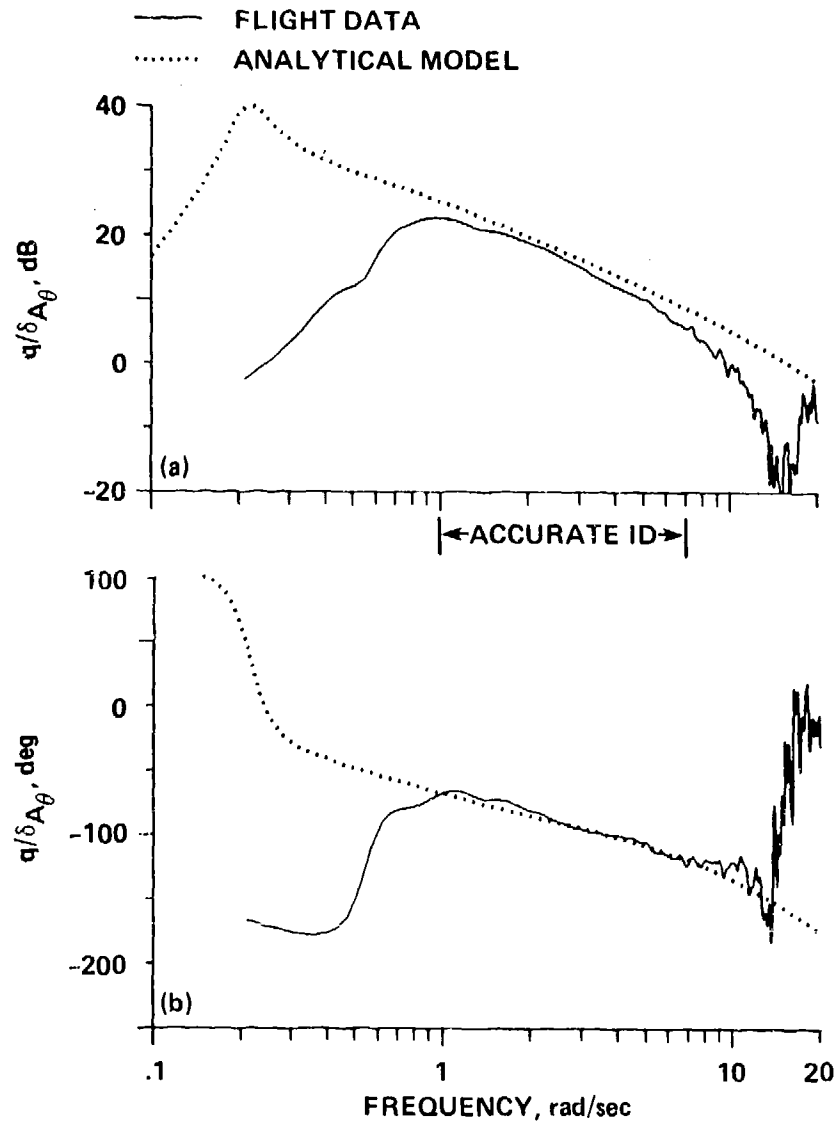

Figure 25.– Open-loop UH-60 response including upper-boost actuator, rotor and rigid body dynamics; (a) magnitude, (b) phase.

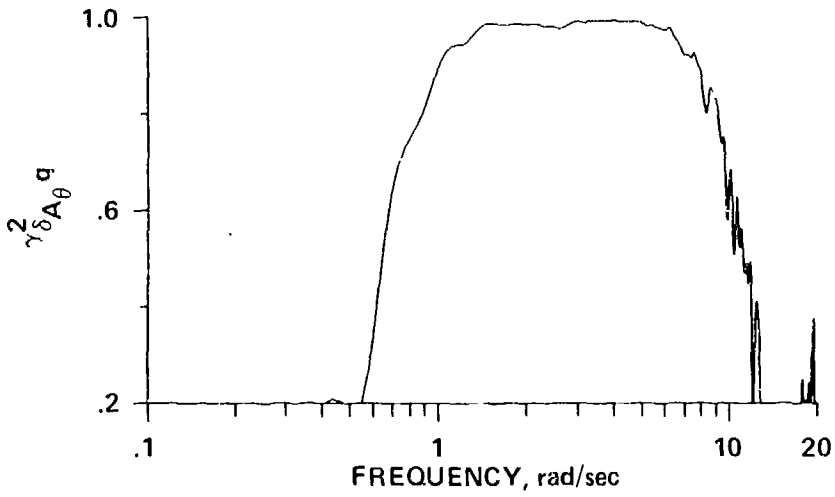

Figure 26.– Coherence for open-loop UH-60 identification.

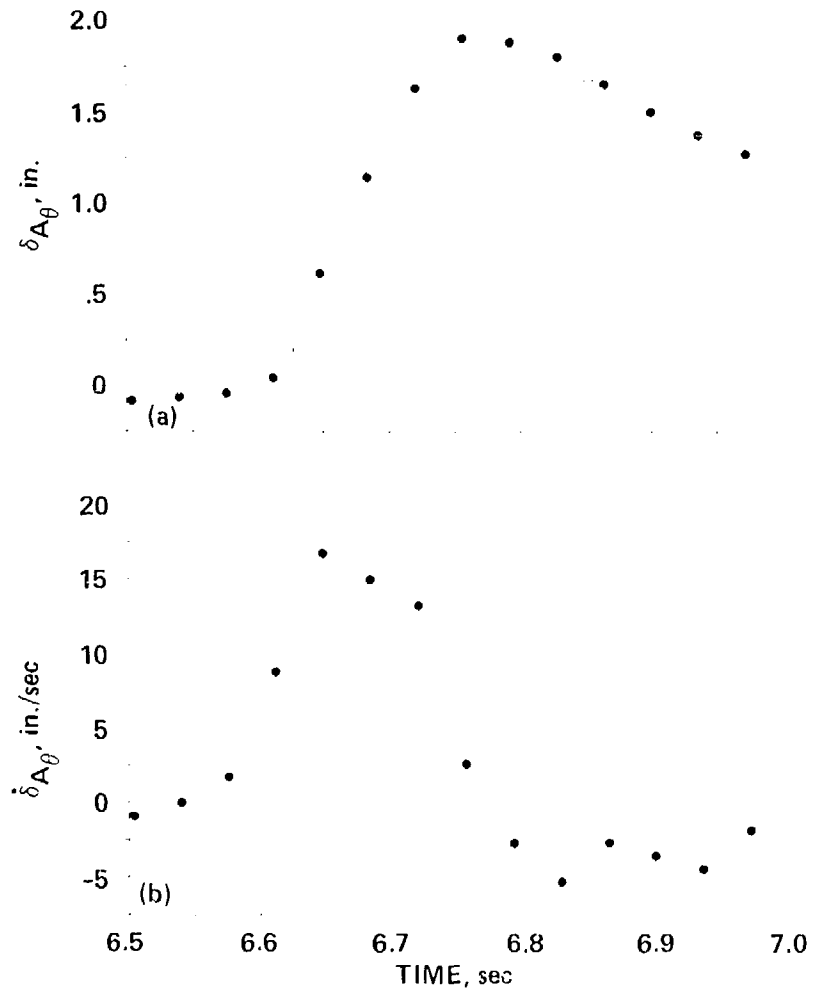

Figure 27.– Flight record of ADOCS filtered actuator response to step longitudinal side-stick input; (a) actuator deflection, (b) calculated actuator rate.

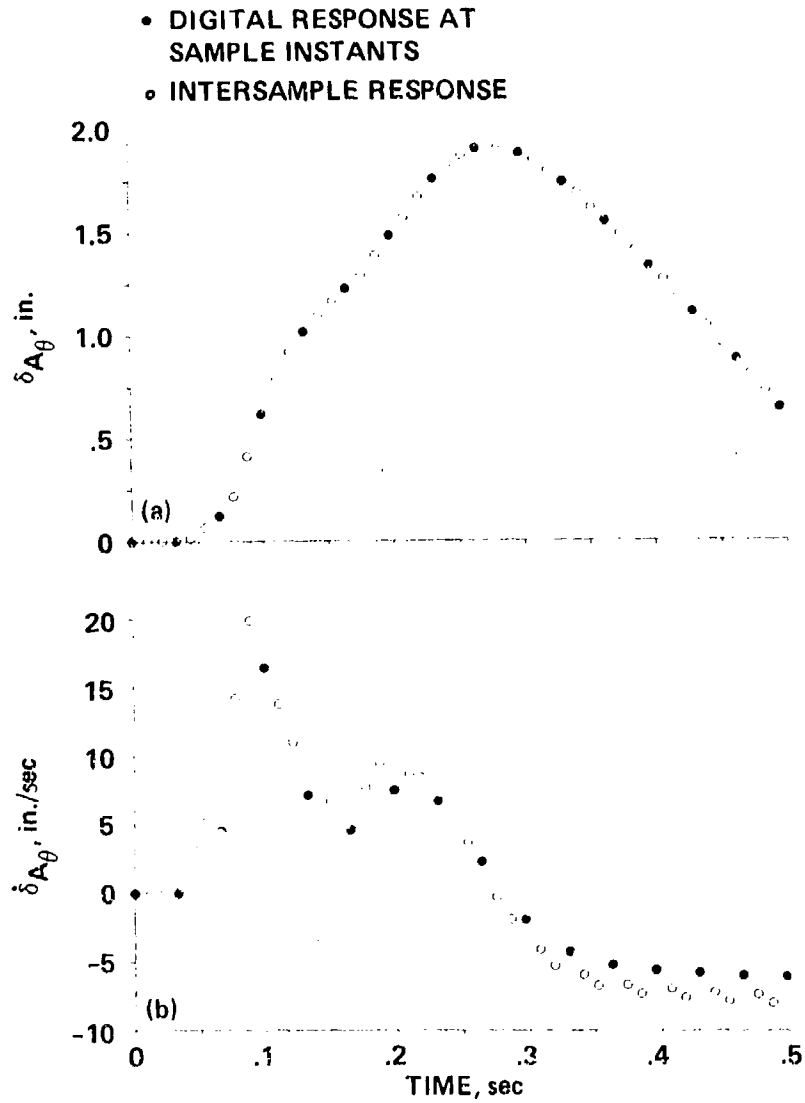

Figure 28.-- Analytical model of ADOCS filtered actuator response to step longitudinal side-stick input; (a) actuator deflection, (b) actuator rate.

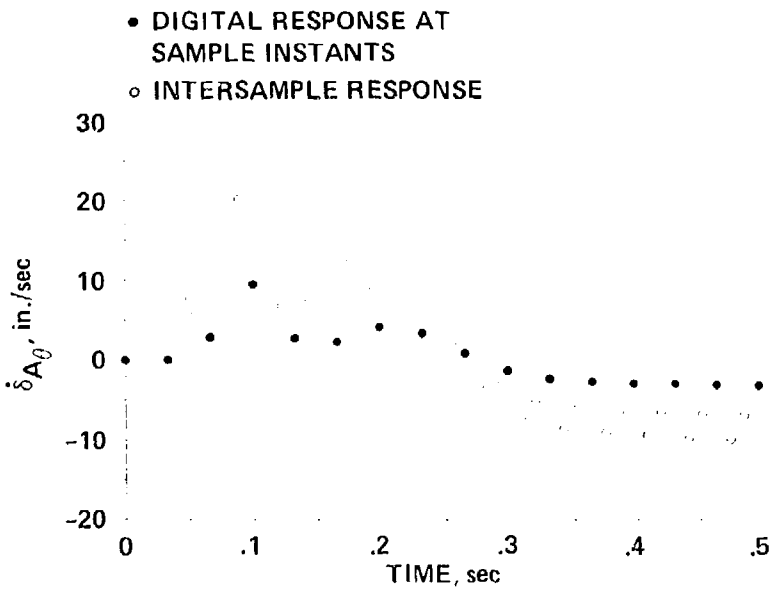

Figure 29.– Analytical model of ADOCS unfiltered actuator rate response to step longitudinal side-stick input.

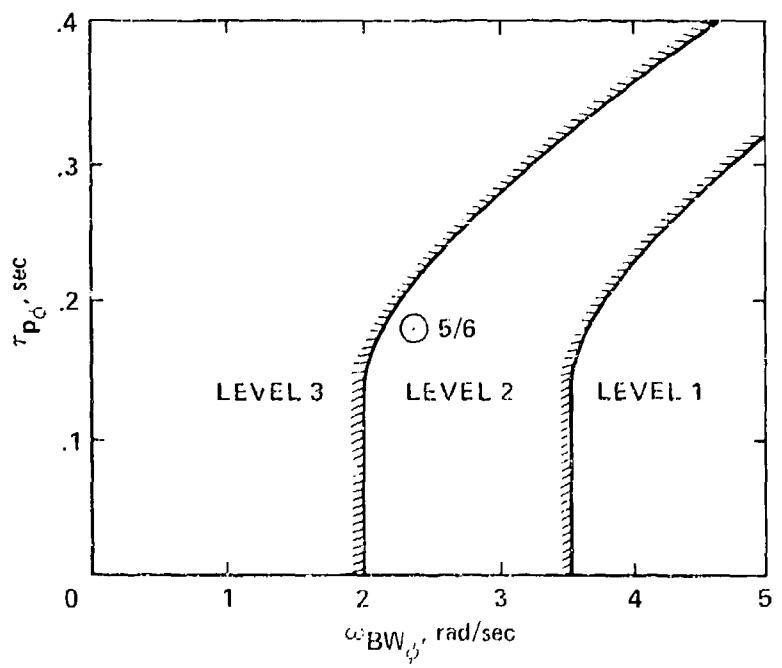

Figure 30.– Handling-qualities correlation of ADOCS roll response in hover for slope landing task (ultra-high gain task). Average ratings are shown for touchdown/lift-off.

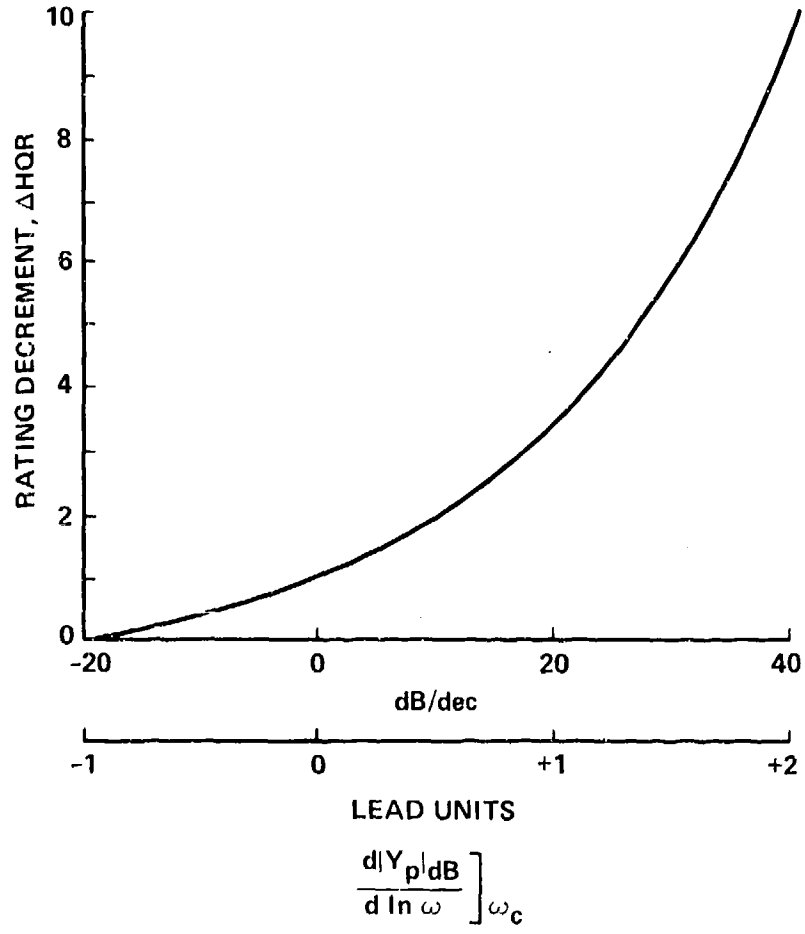

Figure 31.– Pilot rating decrement as a function of lead equalization, reproduced from reference 23.

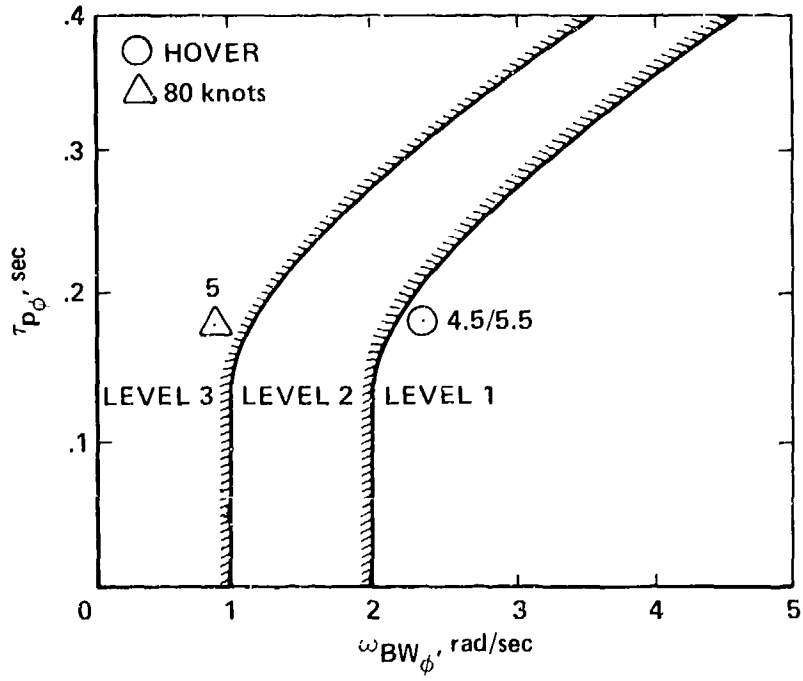

Figure 32.– Handling-qualities correlation of ADOCS roll response in hover and 80 knots. Average ratings are shown only for high-gain roll tasks. (Hover: landing/lift-off; 80 knots: 60 knot-quickstop.)

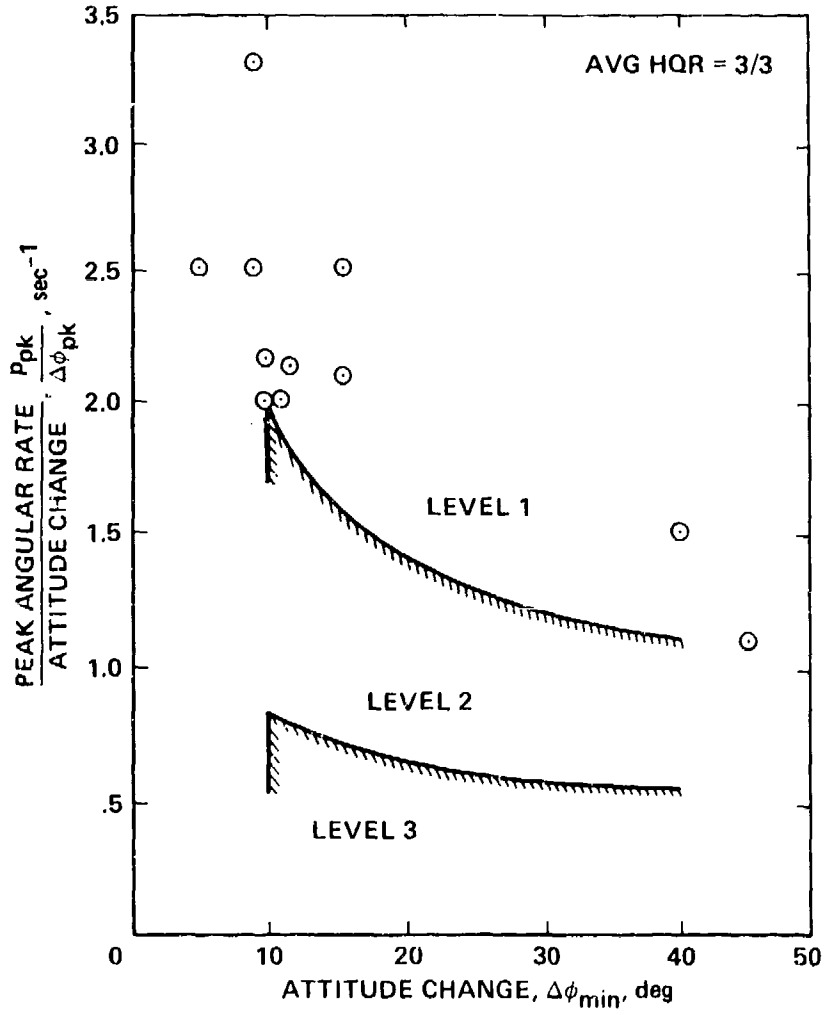

Figure 33.– Handling-qualities correlation of ADOCS moderate amplitude roll response at 80 knots. Average ratings are shown for 180° return-to-target/level roll reversals.

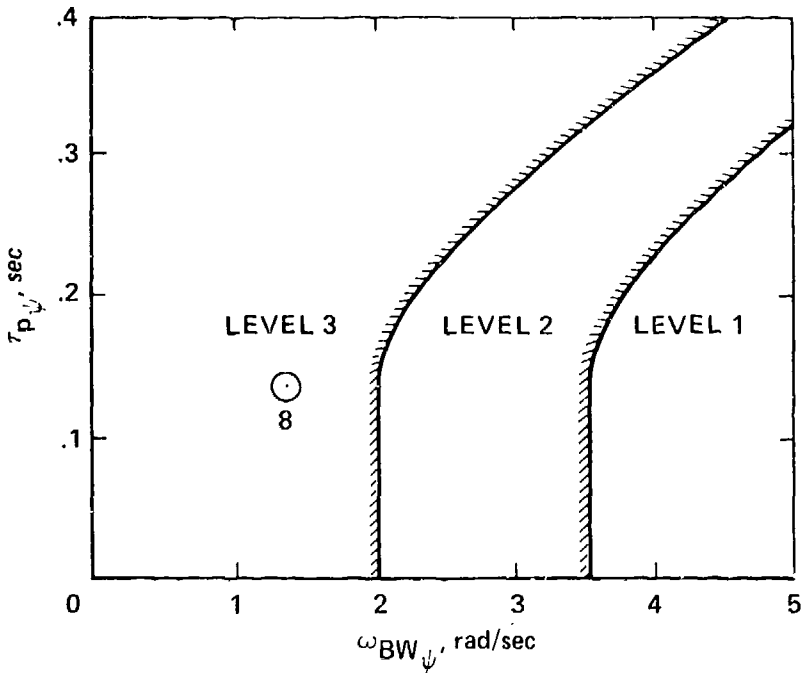

Figure 34.– Handling-qualities correlations of ADOCS yaw response in hover for running landing (ultra-high gain task). Average rating is shown.

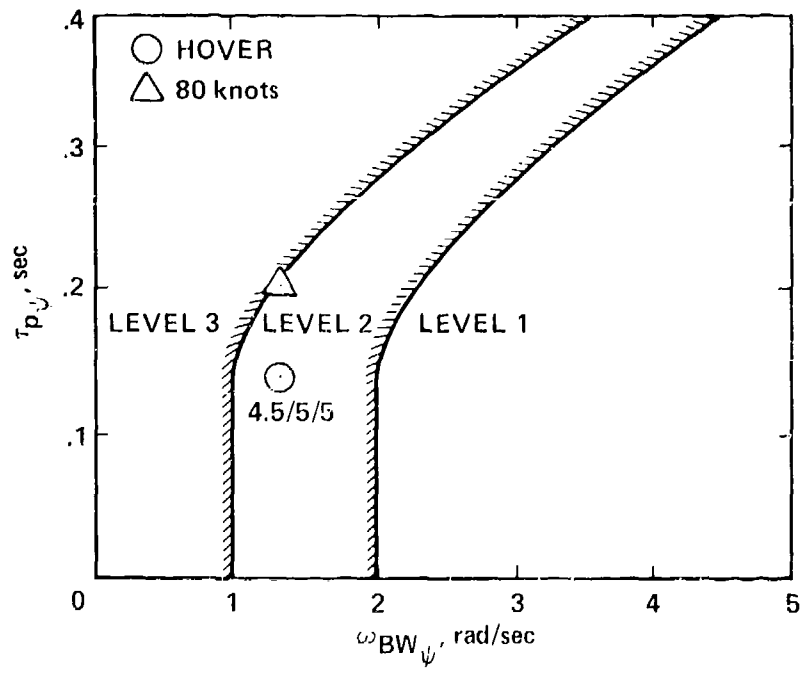

Figure 35.– Handling-qualities correlation of ADOCS yaw in hover and 80 knots. Average ratings are shown only for high-gain yaw tasks (lateral escape/30 knot-slalom/60 knot-quickstop).

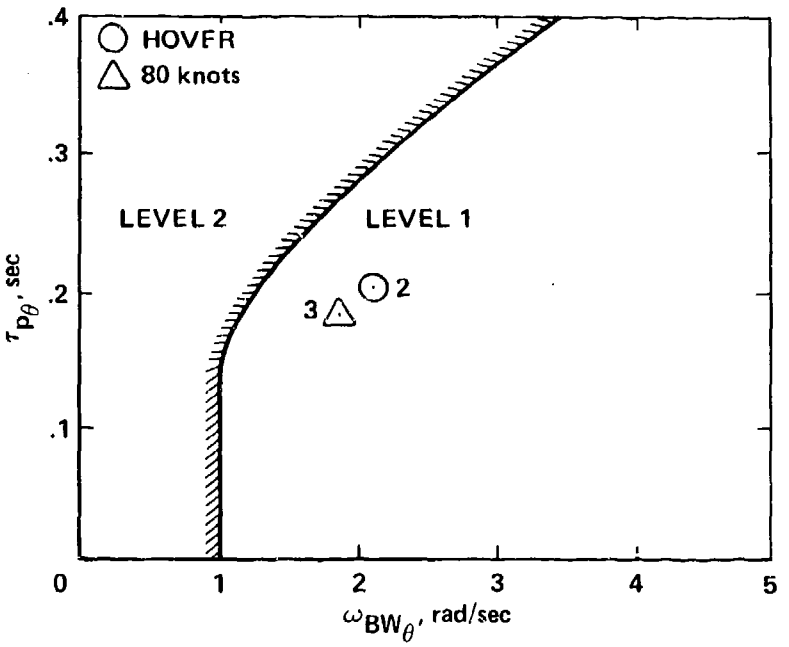

Figure 36.– Handling-qualities correlation of ADOCS pitch response in hover and 80 knots. Average ratings are shown only for low and moderate-gain pitch tasks. (Hover: translations, 80 knots: 180° return-to-target.)

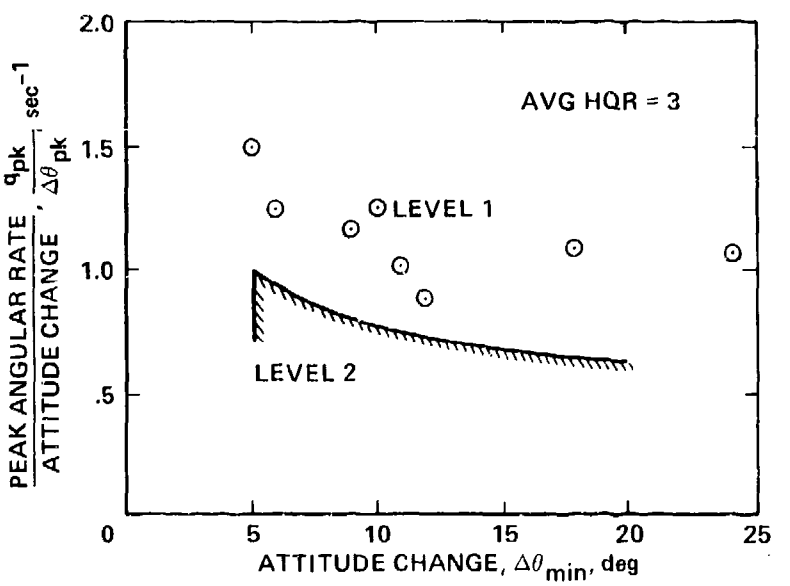

Figure 37.– Handling-qualities correlation of ADOCS moderate amplitude pitch response in hover. Average rating is for initiation of dash.

NASA
National Aeronautics and Space Administration

Report Documentation Page

1. Report No.	2. Government Accession No.	3. Recipient's Catalog No.
NASA TM-101054 USAAVSCOM CP-89-A-002		

4. Title and Subtitle

Applications of Flight Control System Methods to an Advanced Combat Rotorcraft

5. Report Date

July 1989

6. Performing Organization Code

7. Author(s)

Mark B. Tischler, Jay W. Fletcher, Patrick M. Morris,* and George T. Tucker

8. Performing Organization Report No.

A-89006

10. Work Unit No.

992-21-01

9. Performing Organization Name and Address

Ames Research Center, Moffett Field, CA 94035
*Aeroflightdynamics Directorate, U.S. Army Aviation Research and Technology Activity, Ames Research Center, Moffett Field, CA 94035-1099

11. Contract or Grant No.

13. Type of Report and Period Covered

Technical Memorandum

12. Sponsoring Agency Name and Address

National Aeronautics and Space Administration
Washington, DC 20546-0001 and U.S. Army Aviation Systems Command,
St. Louis, MO 63120-1798

14. Sponsoring Agency Code

15. Supplementary Notes

Point of Contact: Mark B. Tischler, Ames Research Center, MS 211-2, Moffett Field, CA 94035
(415) 694-5563 or FTS 464-5563

Report presented at Royal Aeronautical Society International Conference on Helicopter Handling Qualities and Control, London, UK, November 15-17, 1988.

16. Abstract

Advanced flight control system design, analysis, and testing methodologies developed at the Ames Research Center are applied in an analytical and flight test evaluation of the Advanced Digital Optical Control System (ADOCS) demonstrator. The primary objectives of this paper are to describe the knowledge gained about the implications of digital flight control system design for rotorcraft, and to illustrate the analysis of the resulting handling-qualities in the context of the proposed new handling-qualities specification for rotorcraft. Topics covered in-depth are digital flight control design and analysis methods, flight testing techniques, ADOCS handling-qualities evaluation results, and correlation of flight test results with analytical models and the proposed handling-qualities specification.

The evaluation of the ADOCS demonstrator indicates desirable response characteristics based on equivalent damping and frequency, but undesirably large effective time-delays (exceeding 240 msec in all axes). Piloted handling-qualities are found to be desirable or adequate for all low, medium, and high pilot gain tasks; but handling-qualities are inadequate for ultra-high gain tasks such as slope and running landings. Correlation of these results with the proposed handling-qualities specification indicates good agreement for the bandwidth boundaries, but suggests the need for more stringent limits on allowable phase-delay. Analytical models based on emulation (s-plane) techniques compare favorably with flight-extracted frequency-domain characteristics of the overall (end-to-end) ADOCS responses. Direct digital analysis procedures are shown to be necessary to characterize the intersample behavior of the actuator rate response.

17. Key Words (Suggested by Author(s))	18. Distribution Statement
Flight control, Rotorcraft, Flight testing, Handling qualities, Digital control	Unclasssified - Unlimited Subject Category - 08

19. Security Classif. (of this report)	20. Security Classif. (of this page)	21. No. of Pages	22. Price
Unclassified	Unclassified	60	A04

For sale by the National Technical Information Service, Springfield, Virginia 22161